Implicit coupling of heterogeneous and asynchronous time-schemes using a primal approach based on velocity continuity at the subdomain interface

Stéphane Grange, David Bertrand

Version of Record: https://www.sciencedirect.com/science/article/pii/S0168874X21000883
Manuscript_f9a1763643f6b8f4500d769eee552e91

Implicit coupling of heterogeneous and asynchronous time-schemes using a primal approach based on velocity continuity at the subdomain interface

Stéphane Grange, David Bertrand

Univ-Lyon, INSA-Lyon, GEOMAS, EA7495, Villeurbanne, France

Abstract

In the field of structural dynamics, it can be particularly interesting to consider a different time integrator and time scale in a different part of a problem (i.e. in the case of multi-physics problems, non smooth contact mechanics, seismic engineering with impacts, soil-structure interaction problems, or multiscale models using macro-element systems with a dynamic internal equilibrium). This paper presents a primal coupling algorithm based on a velocity gluing at the interface between two subdomains in order to be able to take into account both heterogeneous (different time schemes) and asynchronous (different time steps) time integrations (HATI). This algorithm allows for an implicit nonlinear resolution in providing the exact algorithmic tangent operator to maintain quadratic convergence for Newton-Raphson procedures. It is not intrusive in the finite element code as it only requires an interface element. The algorithm is presented in this paper for coupling different time schemes stemming from both Newmark families and Euler+θ integration schemes (which can be very attractive when dealing with hard contact non smooth mechanics using complementarity methods). The proposed primal approach, which is based on imposing velocity continuity at the interface, is a viable alternative to the classical dual approaches since it is highly suitable for multiscale and sub-structuring models relying on subdomains with internal time integration schemes as well as for problems using macro-element families. The stability analysis exhibits a second order accuracy of the proposed approach. A selection of numerical examples under linear and nonlinear assumptions and for multiple degree-of-freedom system is provided; these examples show that no energy is being dissipated at the interface and overlap very closely with reference solutions.

Keywords:
Heterogeneous, asynchronous, primal coupling based on velocity gluing, Newmark, Euler, implicit, nonlinear, exact tangent operator, static condensation, impact

---

Abbreviations: VPP*, virtual power principle; LCP, linear complementary method; FETI, Finite Element Tearing and Interconnecting; HATI, heterogeneous asynchronous time integrators

1. Introduction

In the framework of finite element analysis and multiscale modelling using sub-structuring techniques, it can be worthwhile to use various integration time integration schemes between two subdomains. Indeed, in multiscale modelling, subdomains, elements or even constitutive laws can have internal degrees of freedom that depend on time and then require use of a time integration scheme to satisfy internal equilibrium. Within a classical framework, when calling these subdomains with a finite element solver (or at the upper scale), it is necessary to ensure that the time integration scheme is the same across all subdomains. This constraint can be very restrictive for the development of time dependent multiscale models or constitutive laws. Moreover, some integration schemes need to be mixed in order to take advantage of the benefits of each. Such is the case, for instance, with the treatment of contact-impact problems (non-smooth contact mechanics), where complementarity methods are classically employed in conjunction with a Euler+θ method, whereas more often structural finite element codes use Newmark family algorithms that are well suited for regular structural dynamics (smooth mechanics).

In the 1970's, several authors proposed mixed time implicit/explicit scheme methods (Liu and Belytschko (1982), Hughes and Liu (1978b), Hughes and Liu (1978a)), with implicit/implicit through interpolation and extrapolation being required on the interface (Belytschko and Mullen (1978), Belytschko et al. (1979)). Such methods present a way to solve a first partition (also called subdomain in this paper) as master and solve a second partition during a second step (slave partition). They are called "primal" Escaig and Marin (1999) and rely on a Schur complement method. These methods typically necessitate conditions to ensure stability. In Smolinski (1992a) and Smolinski (1992b), another explicit time integration coupling was proposed by setting

acceleration conditions in order to maintain stability. More recently, to avoid having to calculate the accelerations (and the condition identified by Smolinski (1992a), Wu and Smolinski (2000)), a method derived from the modified trapezoidal rule method (MTM) was proposed. In Hughes et al. (1979) a coupling is based on predictor and corrector phases and that are built at the beginning for a wave propagation analysis, requiring an explicit algorithm in some parts of structures. Daniel (1997) also proposed a sub-cycling algorithm that averages accelerations. Like previous authors, Klisinski and Moström (1998) suggested an analysis of the stability of these multi-time step integration procedures. In the case of implicit/implicit couplings, no previous work provides any pathway to calculating a tangent operator, as needed in the case of nonlinear problems. In all past papers, the interface continuity condition is applied by gluing a displacement.

Later, several authors proposed alternative coupling algorithms in order to tackle this problem using a Lagrange multiplier at the interface, which characterizes the FETI family method. These methods are called "dual", and the unknowns are the forces at the interface. Farhat et al. (1994), Combescure and Gravouil (2001),Gravouil and Combescure (2001), Combescure and Gravouil (2002) and, more recently Avery and Farhat (2009), Beneš and Kruis (2018), Beneš et al. (2018) and Brun et al. (2015) have all proposed a different means for coupling explicit/implicit subdomains. These methods are very robust and allow running different codes in parallel. Continuity at the interface is ensured by gluing in a velocity, as first introduced by Gravouil and Combescure (2001); they are particularly suitable when subdomains need to be handled in parallel, i.e. at the same modelling level.

Both primal and dual methods are commonly called heterogeneous (different time schemes) and asynchronous (different time steps) time integrators (HATI) for computational structural dynamics; they are presented in a state-of-the-art paper in Gravouil et al. (2015).

The present paper presents a new HATI algorithm based on a primal method and considers continuity at the interface in velocity by duplicating the degrees of freedom at the interface, thus allowing for the potential discontinuity of displacement (and acceleration) at the interface.

The technique proposed here serves to couple implicit time schemes and provides an expression of the resisting force to be returned to the finite element solver by the subdomain that takes into account the characteristics of the time schemes at the interface. This method also yields an exact derivation of the algorithmic tangent operator, thus maintaining the quadratic conver-

gence properties. This layout can be considered as a generalisation of the static condensation of the operators (also called a Schur complement), which is usually presented as an alternative to the FETI method (Escaig and Marin (1999)).

This method is therefore well suited for the formulation of internal kinematic constitutive laws or for macro-elements or materials using internal degrees of freedom in the case of dynamic equilibrium. This technique therefore is not intrusive and only requires a user interface element; moreover, it and can easily be implemented in commercial finite element code.

2. Principle of the primal subdomain and sub-structuring method decompositions

The resolution of the interface problem can be primal (Escaig and Marin (1999)) provided the displacement is the unknown and using a static condensation of the degrees of freedom of one subdomain on a global subdomain. This static condensation is also called a Schur complement.

The resolution of the interface problem can also be dual, whereby the unknowns at the interface are forces, like a Lagrange multiplier, and is called the FETI method.

The primal method can prove to be most beneficial in the case where the subdomain is a macro-element called by a global domain, i.e. if the global domain calls a time dependent element with internal degrees of freedom requiring dynamic equilibrium. Such can also be the case for time-dependent constitutive laws, as in Mazars et al. (2018).

As a very simple initial illustration, let's consider the dynamic equilibrium using a time discretisation, making it possible to express all kinematic quantities (acceleration, velocities, displacement) as a function of just one of them. In the case of problems formulated in displacement, the time scheme used to solve the equation will then provide for every time step $i+1$ a system of the form:

$$\mathbf{P}\left(\mathbf{U}_{i+1}\right) = \tilde{\mathbf{F}}_{i+1} \tag{1}$$

with $\mathbf{P}\left(\mathbf{U}_{i+1}\right)$ being the resisting force and $\tilde{\mathbf{F}}_{i+1}$ the external forces that take into account the time scheme history from the previous time step.

This system can then be linearised using a Newton-Raphson procedure that leads to a tangent operator given by the following relationship:

$$\delta \mathbf{P}_{i+1} = \tilde{\mathbf{K}} \delta \mathbf{U}_{i+1} \tag{2}$$

The operator $\tilde{\mathbf{K}}$ also called the tangent operator, contains all the mechanical quantities originating from the system mass, damping and stiffness of the system linked with the time scheme parameters of the domain.

Let's denote φ and ν the names of the two subdomains to be coupled.

If b denotes the degrees of freedom at the subdomain interface, r^{φ} the internal degrees of freedom of subdomain φ, and r^{ν} the internal degrees of freedom of subdomain ν, then $\mathbf{P}$ and $\tilde{\mathbf{K}}$ can be decomposed into blocks as follows:

$$\mathbf{P} = \begin{bmatrix} \mathbf{P}^{\varphi}_{r^{\varphi}} \\ \mathbf{P}^{\varphi}_{b} + \mathbf{P}^{\nu}_{b} \\ \mathbf{P}^{\nu}_{r^{\nu}} \end{bmatrix} \tag{3}$$

$$\tilde{\mathbf{K}} = \begin{bmatrix} \tilde{\mathbf{K}}_{r^{\varphi}r^{\varphi}} & \tilde{\mathbf{K}}_{r^{\varphi}b} & \mathbf{0} \\ \tilde{\mathbf{K}}_{br^{\varphi}} & \tilde{\mathbf{K}}_{bb} & \tilde{\mathbf{K}}_{br^{\nu}} \\ \mathbf{0} & \tilde{\mathbf{K}}_{br^{\nu}} & \tilde{\mathbf{K}}_{r^{\nu}r^{\nu}} \end{bmatrix} \tag{4}$$

In this case, if we consider that subdomain ν is called by subdomain φ for the global equilibrium, a condensation of the internal equations of subdomain ν must be performed. However, this static condensation can only be carried out by considering the same time scheme used to express both subdomains; otherwise, the blocks of the matrix $\tilde{\mathbf{K}}$, as written in Equation 4, cannot even be collated.

In order to accommodate two different time schemes, a special coupling between the two subdomains is required.

Moreover, in the dynamic case, the nodes must carry not only the displacement information but also velocity and, possibly, acceleration (for second-order time integration schemes).

This paper will thus present a method that consists of splitting the interface nodes, by duplicating them in order to:

- carry the kinematic information of the node in both subdomain φ and subdomain ν;
- impose a kinematic relationship on the displacement, or velocity (or acceleration), at the interface by duplicating the nodes at the interface (see Fig. 1) and applying **a continuity in velocity**;

- compute the adequate resisting force that needs to be returned from subdomain ν to subdomain φ;
- **derive the algorithmic tangent consistent operator** by means of a technique of static condensation.

3. Principle of integration scheme coupling over a single time step

3.1. Introduction

Let φ be a subdomain with a given time scheme and ν another subdomain called by φ with its time scheme.

Whether the time scheme involved is Newmark or Euler+θ (or another scheme, even explicit), the following relationships between displacements, velocities and accelerations (only for a second-order time scheme) at time step $i+1$ can be written as a function of quantities at the previous time step i ($\mathbf{B}_i^{\varphi}$ and $\mathbf{D}_i^{\varphi}$) and time scheme coefficient (A^{φ} and C^{φ}), as defined in table 1.

Thus, the time scheme φ and ν are expressed as follows:

$$\left\{\begin{array}{l}\mathbf{v}_{i+1}^{\varphi} = C^{\varphi}\mathbf{u}_{i+1}^{\varphi} + \mathbf{D}_i^{\varphi} \\ \mathbf{a}_{i+1}^{\varphi} = A^{\varphi}\mathbf{u}_{i+1}^{\varphi} + \mathbf{B}_i^{\varphi}\end{array}\right. \quad and \quad \left\{\begin{array}{l}\mathbf{v}_{i+1}^{\nu} = C^{\nu}\mathbf{u}_{i+1}^{\nu} + \mathbf{D}_i^{\nu} \\ \mathbf{a}_{i+1}^{\nu} = A^{\nu}\mathbf{u}_{i+1}^{\nu} + \mathbf{B}_i^{\nu}\end{array}\right. \tag{5}$$

Table 1 provides an overview of the coefficient values used for time integration families.

Time scheme φ_m	**Constants**	
	Coefficients	**History from previous step**
Newmark	$A^{\varphi_m} = \frac{1}{\beta_m \Delta t_m^2}$ $C^{\varphi_m} = \frac{\gamma_m}{\beta_m \Delta t_m}$	$B_i^{\varphi_m} = -\frac{1}{\beta_m \Delta t_m^2}\left[u_i^{\varphi_m} + \Delta t_m v_i^{\varphi_m} + (\frac{1}{2} - \beta_m)\Delta t_m^2 a_i^{\varphi_m}\right]$ $D_i^{\varphi_m} = -\frac{\gamma_m}{\beta_m \Delta t_m} u_i^{\varphi_m} + (1 - \frac{\gamma_m}{\beta_m})v_i^{\varphi_m} + (1 - \frac{\gamma_m}{2\beta_m})\Delta t_m a_i^{\varphi_m}$
Euler+θ	$A^{\varphi_m} : \{\}$ $C^{\varphi_m} = \frac{1}{\theta_m \Delta t_m}$	$B_i^{\varphi_m} : \{\}$ $D_i^{\varphi_m} = -\frac{1}{\theta_m \Delta t_m}\left[u_i^{\varphi_m} + \Delta t_m\,(1-\theta_m)\,v_i^{\varphi_m}\right]$

Table 1: Parameter values for time scheme integration families

The notion of coupling the 2 subdomains by "duplicating" nodes at the interface to create the interface gluing and a kinematic link and imposing interface continuity is based on the velocities (as proposed in Combescure and Gravouil (2001) for dual couplings). Then, the displacements and accelerations can be calculated within subdomain ν so that this velocity continuity is respected.

The duplicating node is in fact not an additional node. The node is assigned with 2 different kinematic variables depending on whether it is seen by subdomain φ or subdomain ν. The only common kinematic quantity here then is the velocity.

Consequently, imposing velocity continuity at the interface leads to a different displacement and acceleration at the interface of both subdomains. Such is the downside to maintaining this velocity continuity between the 2 subdomains. The kinematic constraint in velocity is thus strictly fulfilled, whereas displacements and accelerations are not strictly fulfilled at the interface.

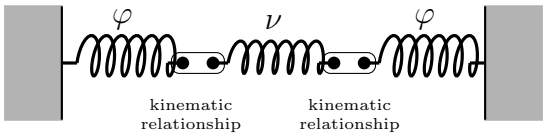

+ for all nodes at the interface
and for every time step:
rigid links: $v_{i+1}^{\varphi} = v_{i+1}^{\nu}$
and links depending on time:
$u^{\nu} = f(u^{\varphi})$ and $a^{\nu} = h(u^{\varphi})$
where f and h are 2 functions
from the time scheme ν.

Figure 1: Illustration of the kinematic links between 2 subdomains incorporating the fact that even if velocities are considered as continuous, the displacements and accelerations are discontinuous at the interfaces.

Imposing velocities between subdomains implies the following relationship:

$$\mathbf{v}_{i+1}^{\varphi} = \mathbf{v}_{i+1}^{\nu} \Leftrightarrow C^{\varphi}\mathbf{u}_{i+1}^{\varphi} + \mathbf{D}_i^{\varphi} = C^{\nu}\mathbf{u}_{i+1}^{\nu} + \mathbf{D}_i^{\nu} \tag{6}$$

From this continuity equation, the displacement to be imposed at the subdomain interface must be:

$$\mathbf{u}_{i+1}^{\nu} = C^{\nu^{-1}}C^{\varphi}\mathbf{u}_{i+1}^{\varphi} + C^{\nu^{-1}}\left(\mathbf{D}_i^{\varphi} - \mathbf{D}_i^{\nu}\right) \tag{7}$$

This same argument can be made in order to derive the accelerations:

$$\begin{aligned} A^{\nu^{-1}}\left(\mathbf{a}_{i+1}^{\nu} - \mathbf{B}_i^{\nu}\right) &= C^{\nu^{-1}}C^{\varphi}A^{\varphi^{-1}}\left(\mathbf{a}_{i+1}^{\varphi} - \mathbf{B}_i^{\varphi}\right) + C^{\nu^{-1}}\left(\mathbf{D}_i^{\varphi} - \mathbf{D}_i^{\nu}\right) \\ \Leftrightarrow \mathbf{a}_{i+1}^{\nu} &= A^{\nu}C^{\nu^{-1}}C^{\varphi}A^{\varphi^{-1}}\mathbf{a}_{i+1}^{\varphi} + A^{\nu}C^{\nu^{-1}}\left(\mathbf{D}_i^{\varphi} - \mathbf{D}_i^{\nu}\right) - A^{\nu}C^{\nu^{-1}}C^{\varphi}A^{\varphi^{-1}}\mathbf{B}_i^{\varphi} + \mathbf{B}_i^{\nu} \end{aligned} \tag{8}$$

*3.2. Resisting force at the interface between subdomains: Equilibrium equations using the virtual power principle VPP**

The VPP* applied with a virtual field proportional to the velocities allows projecting onto a continuous kinematic field at the interface.

Let's consider the following resisting forces at the boundary of two subdomains (formulated in displacements): $\mathbf{F}^{\varphi}\left(\mathbf{u}_{i+1}^{\varphi}, \mathbf{v}_{i+1}^{\varphi}, \mathbf{a}_{i+1}^{\varphi}\right)$, the internal resisting force originating from subdomain φ at the interface nodes; and $\mathbf{F}^{\nu}\left(\mathbf{u}_{i+1}^{\nu}, \mathbf{v}_{i+1}^{\nu}, \mathbf{a}_{i+1}^{\nu}\right)$, the internal resisting force originating from subdomain ν at the interface nodes.

The VPP* can thus be expressed as follows (where f, g, and h are the time scheme-dependent functions):

$$\begin{aligned} &\forall \mathbf{v}^*,\ {}^t\mathbf{v}_{i+1}^{\varphi^*}\mathbf{F}^{\varphi}\left(\mathbf{u}_{i+1}^{\varphi}, \mathbf{v}_{i+1}^{\varphi}, \mathbf{a}_{i+1}^{\varphi}\right) + {}^t\mathbf{v}_{i+1}^{\nu^*}\mathbf{F}^{\nu}\left(\mathbf{u}_{i+1}^{\nu}, \mathbf{v}_{i+1}^{\nu}, \mathbf{a}_{i+1}^{\nu}\right) = 0 \\ \Leftrightarrow\ &\forall \mathbf{v}^*,\ {}^t\mathbf{v}_{i+1}^{\varphi^*}\mathbf{F}^{\varphi}\left(\mathbf{u}_{i+1}^{\varphi}, \mathbf{v}_{i+1}^{\varphi}, \mathbf{a}_{i+1}^{\varphi}\right) + {}^t\mathbf{v}_{i+1}^{\varphi^*}\mathbf{F}^{\nu}\left(f(\mathbf{u}_{i+1}^{\varphi}), g(\mathbf{u}_{i+1}^{\varphi}), h(\mathbf{u}_{i+1}^{\varphi})\right) = 0 \end{aligned} \tag{9}$$

In the second part of equation 9, the internal kinematics of subdomain φ can be easily written from the displacement $\mathbf{u}_{i+1}^{\varphi}$-dependent velocities and accelerations.

From the fact that velocity continuity is respected $\mathbf{v}_{i+1}^{\varphi^*} = \mathbf{v}_{i+1}^{\nu^*}$, it is not necessary to modify the internal resisting force from subdomain ν to φ.

In this paper, this internal resisting force at the interface is assumed to be regular enough to compute the algorithmic tangent operator, which means that if a discontinuity field were to be considered, it would have to be considered within the subdomain and not at its boundary.

3.3. Algorithmic tangent operator required when using an implicit scheme

In order to maintain quadratic convergence, a time connection factor between the time integration schemes is needed to calculate exactly the algorithmic tangent operator.

The motivation for computing this algorithmic tangent operator is to ensure the best possible convergence when using the Newton Raphson's global strategy by coupling subdomains ν and φ (i.e. the same convergence obtained if the same time schemes and time steps were used in the both subdomains). This algorithmic tangent operator ensures for example that the convergence of the coupling between 2 linear elastic subdomains with different time steps is achieved in 1 iteration. It also ensures, for nonlinear behaviour, that the coupling does not generate additional iterations (compared to the case with the same time schemes in both subdomains).

In the case where subdomain ν is not able to return an exact tangent stiffness (e.g. damage behaviour constitutive laws, which is usually secant stiffness, and in other cases only the initial stiffness can be provided if the tangent stiffness is not definite), then the secant or initial stiffness matrix provided by subdomain ν can be used. This term of algorithmic "tangent" operator is introduced to point out the fact that the coupling algorithm operator does not degrade convergence, depending on what is best provided by the subdomain ν.

The demonstration is first proposed in the case where the time scheme of subdomain φ is written in displacement; the derivatives of the internal forces must thus be taken with respect to displacement. However, this same kind of demonstration can be performed with time schemes written in velocity (or acceleration) by adapting the derivation steps.

In the following subsections, a simple demonstration is initially offered and only valid for mono-time stepping (Section 3.3.1), while a second demonstration establishes the basics of a more powerful derivation for multi-time stepping algorithms (Section 3.3.2), which will be treated in Section 4.

3.3.1. A simple demonstration of the tangent operator with mono-time stepping

The algorithmic tangent operator to be returned (originating from subdomain ν) to subdomain φ is written (at time step $i+1$) as follows and moreover can be obtained by the composite derivatives of the resisting force at the interface.

$$\frac{\partial \mathbf{F}^{\nu}_{i+1}}{\partial \mathbf{u}^{\varphi}_{i+1}} = \frac{\partial \mathbf{F}^{\nu}_{i+1}}{\partial \mathbf{u}^{\nu}_{i+1}} \frac{\partial \mathbf{u}^{\nu}_{i+1}}{\partial \mathbf{u}^{\varphi}_{i+1}} \tag{10}$$

A factor, possibly called the time connection factor, between the 2 subdomains can be easily derived by writing a variation of Equation 7 linking the displacements to the subdomains.

In knowing the tangent operator of subdomain ν (as necessarily provided by subdomain ν in its internal resolution $\frac{\partial \mathbf{F}^{\nu}_{i+1}}{\partial \mathbf{u}^{\nu}_{i+1}} = \tilde{\mathbf{k}}$), then the algorithmic tangent operator to be returned to subdomain φ is equal to:

$$\frac{\partial \mathbf{F}^{\nu}_{i+1}}{\partial \mathbf{u}^{\varphi}_{i+1}} = \tilde{\mathbf{k}}\ C^{\nu^{-1}} C^{\varphi} \tag{11}$$

Note:. The same demonstration can be made if subdomain φ is written with velocity or acceleration as its principal variable by expressing the differentiation of the internal resisting force with $\mathbf{v}_{i+1}^{\varphi}$ or $\mathbf{a}_{i+1}^{\varphi}$).

Next, in a more general manner, if subdomain φ is written with kinematic $\mathbf{w}_{i+1}^{\varphi}$ and subdomain ν with $\mathbf{z}_{i+1}^{\nu}$ (w and z can be either displacement, velocity or acceleration), the algorithmic tangent operator can be written as:

$$\frac{\partial \mathbf{F}_{i+1}^{\nu}}{\partial \mathbf{w}_{i+1}^{\varphi}} = \frac{\partial \mathbf{F}_{i+1}^{\nu}}{\partial \mathbf{z}_{i+1}^{\nu}} \frac{\partial \mathbf{z}_{i+1}^{\nu}}{\partial \mathbf{w}_{i+1}^{\varphi}} = \tilde{\mathbf{k}} \frac{\partial \mathbf{z}_{i+1}^{\nu}}{\partial \mathbf{w}_{i+1}^{\varphi}} \tag{12}$$

3.3.2. A more general demonstration of the algorithmic tangent operator

To derive the tangent operator more elegantly and for a more complex demonstration in multi-time stepping by an appropriate static condensation, it is necessary to decompose the force and displacement vectors into an internal part (for the ν subdomain) and a part of nodes at the interface with subdomain φ. This decomposition will yield an exact calculation of the tangent operator in multi-time steps and demonstrate the algorithmic static condensation to be returned. The decomposition of these 2 sets of kinematic and force variables is shown in Figure 2.

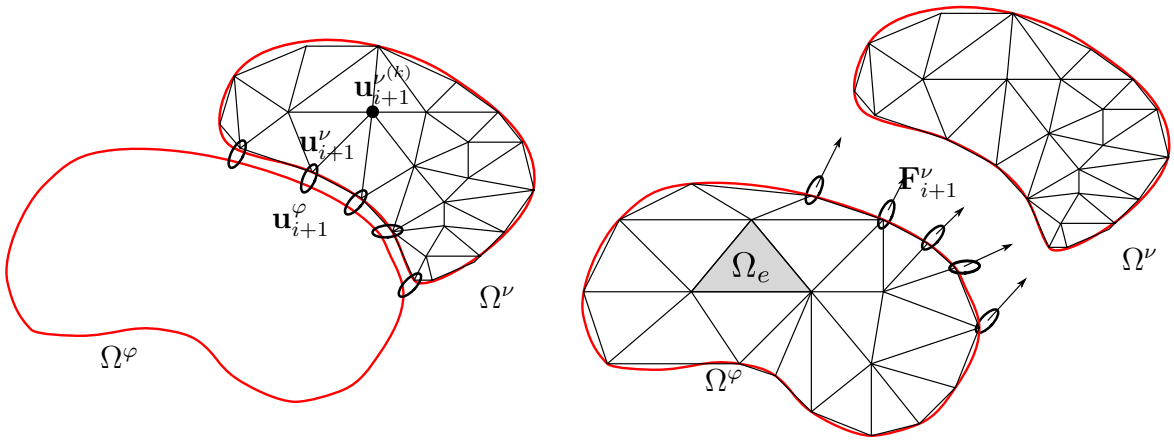

Figure 2: Representation of the links between kinematics at the interface of subdomains ($\mathbf{u}_{i+1}^{\varphi}$ and $\mathbf{u}_{i+1}^{\nu}$) and inside subdomain ν ($\mathbf{u}_{i+1}^{\nu^{(k)}}$) for the internal resolution, and resisting forces ($\mathbf{F}_{i+1}^{\nu}$) originating from the subdomain ν at the interface and to be returned to subdomain φ

Notation used in the following:. We can therefore write the global force vector of the ν subdomain (g=global) $\mathbf{F}_{i+1}^{g\nu}$ originating from the assembly of subdomain ν (b=degrees of freedom at the interface between φ and ν and r=internal degrees of freedom of ν). The forces at the interface are denoted $\mathbf{F}_{i+1}^{\nu}$ whereas the forces inside the subdomain are denoted $\mathbf{F}_{i+1}^{\nu^{(k)}}$

$$\mathbf{F}_{i+1}^{g\nu} = \left[\begin{array}{c} \mathbf{f}_b \\ \mathbf{f}_r \end{array} \right] = \left[\begin{array}{c} \mathbf{F}_{i+1}^{\nu} \\ \mathbf{F}_{i+1}^{\nu^{(k)}} \end{array} \right] \tag{13}$$

Regarding the kinematic variables: $\mathbf{u}_{i+1}^{\varphi}$ and $\mathbf{u}_{i+1}^{\nu}$ are located at the interface between the 2 subdomains and $\mathbf{u}_{i+1}^{\nu^{(k)}}$ is located inside subdomain ν (internal degrees of freedom).

$$\mathbf{U}_{i+1}^{\nu} = \left[\begin{array}{c} \mathbf{u}_b \\ \mathbf{u}_r \end{array} \right] = \left[\begin{array}{c} \mathbf{u}_{i+1}^{\nu} \\ \mathbf{u}_{i+1}^{\nu^{(k)}} \end{array} \right] \tag{14}$$

For the sake of simplicity, in the following, subscripts e and i have been omitted. All quantities at the interface of subdomains $\mathbf{X}_b$ and inside subdomains $\mathbf{X}_r$ are respectively replaced at time $i+1$ for subdomain m by $\mathbf{X}_{i+1}^{\varphi_m}$ and $\mathbf{X}_{i+1}^{\varphi_m^{(k)}}$. The superscript g has been retained for the global resisting force (interface and internal nodes), and uppercase letters are used to indicate the global kinematic variables (displacements, velocities, accelerations).

By imposing the kinematic relationship at the interface ($\mathbf{u}_{i+1}^{\nu}$), which stands for displacements, the global displacement vector collecting all degrees of freedom of subdomain ν is written:

$$\mathbf{U}_{i+1}^{\nu} = \left[\begin{array}{c} \mathbf{u}_b \\ \mathbf{u}_r \end{array} \right] = \left[\begin{array}{c} \mathbf{u}_{i+1}^{\nu} \\ \mathbf{u}_{i+1}^{\nu^{(k)}} \end{array} \right] = \left[\begin{array}{c} C^{\nu^{-1}} C^{\varphi} \mathbf{u}_{i+1}^{\varphi} \\ \mathbf{u}_{i+1}^{\nu^{(k)}} \end{array} \right] \tag{15}$$

The internal dynamic equation given by the global resisting force is (depending on the displacements, velocities and accelerations of all the nodes of subdomain ν): $\mathbf{F}_{i+1}^{g\nu} = \mathbf{F}^{g\nu}\left(\mathbf{U}_{i+1}^{\nu}, \mathbf{V}_{i+1}^{\nu}, \mathbf{A}_{i+1}^{\nu}\right)$. For implicit/implicit couplings, this latter can be linearised (or at least roughly evaluated inside the resolution of subdomain ν, because it is the one used in the dynamic equilibrium by means of a Newton Raphson procedure of subdomain ν).

Hence, a linearisation (or an approximation used to solve for the equilibrium of subdomain ν according to the following steps) of the global resisting

force can always be performed as:

$$d\mathbf{F}^{g\nu}\left(\mathbf{U}_{i+1}^{\nu},\mathbf{V}_{i+1}^{\nu},\mathbf{A}_{i+1}^{\nu}\right)=\mathbf{M}d\mathbf{A}_{i+1}^{\nu}+\mathbf{C}d\mathbf{V}_{i+1}^{\nu}+\mathbf{K}d\mathbf{U}_{i+1}^{\nu} \tag{16}$$

Note:. All matrices can be written by sub-structuring internal and interface degrees of freedom; also, **at convergence**, $\delta\mathbf{F}_{i+1}^{\nu^{(k)}}$ vanishes (internal equilibrium of the internal nodes), yielding:

$$\begin{array}{r}\left[\begin{array}{cc}\mathbf{M}_{bb} & \mathbf{M}_{br}\\ \mathbf{M}_{rb} & \mathbf{M}_{rr}\end{array}\right]\left[\begin{array}{c}d\mathbf{a}_{i+1}^{\nu}\\ d\mathbf{a}_{i+1}^{\nu^{(k)}}\end{array}\right]+\left[\begin{array}{cc}\mathbf{C}_{bb} & \mathbf{C}_{br}\\ \mathbf{C}_{rb} & \mathbf{C}_{rr}\end{array}\right]\left[\begin{array}{c}d\mathbf{v}_{i+1}^{\nu}\\ d\mathbf{v}_{i+1}^{\nu^{(k)}}\end{array}\right]+\cdots\\ \cdots+\left[\begin{array}{cc}\mathbf{K}_{bb} & \mathbf{K}_{br}\\ \mathbf{K}_{rb} & \mathbf{K}_{rr}\end{array}\right]\left[\begin{array}{c}d\mathbf{u}_{i+1}^{\nu}\\ d\mathbf{u}_{i+1}^{\nu^{(k)}}\end{array}\right]=\left[\begin{array}{c}d\mathbf{F}_{i+1}^{\nu}\\ 0\end{array}\right]\end{array} \tag{17}$$

At this point, using the time scheme discretisation of subdomain ν, which is valid for the internal degrees of freedom as well as the degrees of freedom at the interface between the subdomains, we obtain the following:

$$\left\{\begin{array}{l}\mathbf{A}_{i+1}^{\nu}=A^{\nu}\mathbf{U}_{i+1}^{\nu}+\mathbf{B}_{i}^{g\nu}\\ \mathbf{V}_{i+1}^{\nu}=C^{\nu}\mathbf{U}_{i+1}^{\nu}+\mathbf{D}_{i}^{g\nu}\end{array}\right. \tag{18}$$

By differentiating these expressions (in knowing that the quantities at time step i are constant, which will not be the case for multi-time stepping):

$$\left\{\begin{array}{l}d\mathbf{A}_{i+1}^{\nu}=A^{\nu}d\mathbf{U}_{i+1}^{\nu}\\ d\mathbf{V}_{i+1}^{\nu}=C^{\nu}d\mathbf{U}_{i+1}^{\nu}\end{array}\right. \tag{19}$$

Then, the classical relationship is derived for the algorithmic operator at the global level:

$$d\mathbf{F}_{i+1}^{g\nu}=\underbrace{\left(\mathbf{M}A^{\nu}+\mathbf{C}C^{\nu}+\mathbf{K}\right)}_{\tilde{\mathbf{K}}}d\mathbf{U}_{i+1}^{\nu} \tag{20}$$

In this previous relationship, $\tilde{\mathbf{K}}$ is the global algorithmic tangent operator of subdomain ν (with all the degrees of freedom of the subdomain: i.e. internal degrees of freedom plus those at the interface).

Then:

$$\left[\begin{array}{c}d\mathbf{F}_{i+1}^{\nu}\\ d\mathbf{F}_{i+1}^{\nu^{(k)}}\end{array}\right]=\tilde{\mathbf{K}}\left[\begin{array}{c}d\mathbf{u}_{i+1}^{\nu}\\ d\mathbf{u}_{i+1}^{int\nu}\end{array}\right]=\tilde{\mathbf{K}}\left[\begin{array}{c}C^{\nu^{-1}}C^{\varphi}d\mathbf{u}_{i+1}^{\varphi}\\ d\mathbf{u}_{i+1}^{\nu^{(k)}}\end{array}\right] \tag{21}$$

At internal convergence of the subdomain ν, the residual equals 0 and the internal forces vanish leaving: $\mathbf{F}_{i+1}^{\nu^{(k)}} = -\mathbf{R}_{i+1}^{\nu^{(k)}} = \mathbf{0}$, so that: $\delta\mathbf{F}_{i+1}^{\nu^{(k)}} = \mathbf{0}$.

A simple static condensation of the 2nd equation of this system can thus be operated on the first equation to obtain:

$$\mathbf{0} = \tilde{\mathbf{K}}_{rb} C^{\nu^{-1}} C^{\varphi} d\mathbf{u}_{i+1}^{\varphi} + \tilde{\mathbf{K}}_{rr} d\mathbf{u}_{i+1}^{\nu^{(k)}} \tag{22}$$

and input into the first equation:

$$d\mathbf{F}_{i+1}^{\nu} = \left[\tilde{\mathbf{K}}_{bb} C^{\nu^{-1}} C^{\varphi} - \tilde{\mathbf{K}}_{br} \tilde{\mathbf{K}}_{rr}^{-1} \tilde{\mathbf{K}}_{rb} C^{\nu^{-1}} C^{\varphi}\right] d\mathbf{u}_{i+1}^{\varphi} \tag{23}$$

Then:

$$d\mathbf{F}_{i+1}^{\nu} = \underbrace{\left[\tilde{\mathbf{K}}_{bb} - \tilde{\mathbf{K}}_{br} \tilde{\mathbf{K}}_{rr}^{-1} \tilde{\mathbf{K}}_{rb}\right]}_{\tilde{\mathbf{k}}} C^{\nu^{-1}} C^{\varphi} d\mathbf{u}_{i+1}^{\varphi} \tag{24}$$

Ultimately, this demonstration shows that the internal stiffness matrix of subdomain ν must be multiplied by the time connection factor between the both time schemes, i.e.: $C^{\nu^{-1}} C^{\varphi}$.

This same demonstration can be performed if the principal variable of the subdomains is the velocity or the acceleration.

4. Coupling between 2 subdomains with different time schemes and with a multi-time stepping

If the time scheme of subdomain ν has a smaller time step than the time scheme of subdomain φ, according to the literature and particularly the FETI method, the velocity can be interpolated linearly at the interface of the subdomains from the beginning to the end of the coarse time step Combescure and Gravouil (2001); Brun et al. (2015).

Let i be the time step number of subdomain φ (time step dt_{φ}) and p the fine time step of subdomain ν (time step dt_{ν}).

Let's also consider that the coarse time step has been divided into an integer number m of time steps dt_{ν}:

$$dt_{\varphi} = m dt_{\nu}; \tag{25}$$

The evolution of the velocity for subdomain ν at its interface over the coarse time step in subdomain φ is therefore written (with $\lambda_p \in [0, 1]$) as proposed in Combescure and Gravouil (2001):

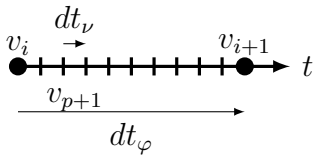

Figure 3: Interpolation of the velocity inside subdomain ν with fine time step $p+1$ at the interface of subdomain φ with coarse time step $i+1$

$$\mathbf{v}_{p+1}^{\nu} = \lambda_{p+1}\mathbf{v}_{i+1}^{\varphi} + \lambda_p \mathbf{v}_i^{\varphi} \tag{26}$$

This development means that the time connection at the interface between subdomains is still completely controlled by velocity. Displacements and accelerations can be deduced in a similar manner as before, as follows:

$$\begin{cases} \mathbf{u}_{p+1}^{\nu} = C^{\nu^{-1}}\left(\mathbf{v}_{p+1}^{\nu} - \mathbf{D}_p^{\nu}\right) \\ \mathbf{a}_{p+1}^{\nu} = A^{\nu}\mathbf{u}_{p+1}^{\nu} + \mathbf{B}_p^{\nu} \end{cases} \tag{27}$$

At each fine time step $p+1$, the new kinematic indicated above, which must be imposed at the interface of subdomain ν, is calculated as many times as there are internal time steps in the step between i and $i+1$.

4.1. Resisting forces at the interface between subdomains

Resisting force $\mathbf{F}^{\nu}\left(\mathbf{u}_{p+1}^{\nu}, \mathbf{v}_{p+1}^{\nu}, \mathbf{a}_{p+1}^{\nu}\right)$ is calculated in this loop by updating the trajectory imposed by the linear interpolation of velocity, as well as by updating the internal variables.

At the end of the sequence of the N time steps, the resisting force $\mathbf{F}^{\nu}\left(\mathbf{u}_{p+1}^{\nu}, \mathbf{v}_{p+1}^{\nu}, \mathbf{a}_{p+1}^{\nu}\right)$ is obtained when $\mathbf{v}_{p+1}^{\nu} = \mathbf{v}_{i+1}^{\varphi}$ yielding the resisting force returned to subdomain φ.

The VPP* then gives the following (where f, g, and h are the time scheme-dependent functions):

$$\begin{aligned} &\forall \mathbf{v}^*,\ {}^t\mathbf{v}_{i+1}^{\varphi^*}\mathbf{F}^{\varphi}\left(\mathbf{u}_{i+1}^{\varphi}, \mathbf{v}_{i+1}^{\varphi}, \mathbf{a}_{i+1}^{\varphi}\right) + {}^t\mathbf{v}_{p+1}^{\nu^*}\mathbf{F}^{\nu}\left(\mathbf{u}_{p+1}^{\nu}, \mathbf{v}_{p+1}^{\nu}, \mathbf{a}_{p+1}^{\nu}\right) = 0 \\ \Leftrightarrow\ &\forall \mathbf{v}^*,\ {}^t\mathbf{v}_{i+1}^{\varphi^*}\mathbf{F}^{\varphi}\left(\mathbf{u}_{i+1}^{\varphi}, \mathbf{v}_{i+1}^{\varphi}, \mathbf{a}_{i+1}^{\varphi}\right) + {}^t\mathbf{v}_{i+1}^{\varphi^*}\mathbf{F}^{\nu}\left(f(\mathbf{u}_{i+1}^{\varphi}), g(\mathbf{u}_{i+1}^{\varphi}), h(\mathbf{u}_{i+1}^{\varphi})\right) = 0 \end{aligned} \tag{28}$$

Here again, resisting force $\mathbf{F}^{\nu}$ does not require modification to be introduced into the equilibrium equation because ${}^t\mathbf{v}_{p+1}^{\nu^*} = {}^t\mathbf{v}_{i+1}^{\varphi^*}$.

4.2. Algorithmic tangent operator for implicit schemes

The subdivision of time steps is actually not so straightforward in the case of an implicit scheme for multi-time stepping couplings, whose tangent operator must be derived in order to maintain quadratic convergence. Indeed, the evolution of resisting force $\mathbf{F}^{\nu}$ must be taken into account throughout the fine time steps dt_2 over dt_1 to correctly compute the algorithmic tangent operator, defined as:

$$\tilde{\mathbf{k}}_{p+1} = \frac{\partial \mathbf{F}^{\nu}_{p+1}}{\partial \mathbf{u}^{\varphi}_{i+1}} \tag{29}$$

This operator (which will be calculated in the next subsection) is defined at the last fine time step $p+1$, when the velocity ultimately coincides with the velocity of the time step $i+1$ in subdomain φ:

The difficulty of calculating the derivative of $\mathbf{F}^{\nu}_{p+1}$ with respect to $\mathbf{u}^{\varphi}_{i+1}$ lies in the fact the resisting force varies with the evolution in the internal kinematic variables of subdomain ν. The internal equilibrium equation at each time step $p+1$ evolves in accordance with the previous step's kinematics (time step p). This relationship can no longer be explicitly given.

4.2.1. Internal equilibrium equation linearisation

To find the appropriate static condensation at each time step $p+1$, it is necessary to incorporate the variation of the internal equilibrium equation for every fine time step $p+1$.

For every call to subdomain ν (N times on the loop over $p+1$ index, which varies from 1 to N), the internal Newton iterations (on (k)) of subdomain ν make it possible to converge towards an internal equilibrium equation given by the residual $\mathbf{R}^{(k)}_{p+1} = 0$.

The global resisting force vector of subdomain ν, derived from the assembly of subdomain ν, is written as (b=dofs at the interface and r=internal dofs):

$$\mathbf{F}^{g\nu}_{p+1} = \begin{bmatrix} \mathbf{f}_b \\ \mathbf{f}_r \end{bmatrix} = \begin{bmatrix} \mathbf{F}^{\nu}_{p+1} \\ \mathbf{F}^{\nu(k)}_{p+1} \end{bmatrix} = \begin{bmatrix} \mathbf{F}^{\nu}_{p+1} \\ -\mathbf{R}^{(k)}_{p+1} \end{bmatrix} \tag{30}$$

Note: The residual term $\mathbf{R}^{(k)}_{p+1}$ obviously contains the internal forces of subdomain ν, yet it also contains the external body or surface forces of the subdomain.

The displacements from subdomain ν can be written as:

$$d\mathbf{U}_{p+1}^{\nu} = \left[\begin{array}{c} d\mathbf{u}_b \\ d\mathbf{u}_r \end{array} \right] = \left[\begin{array}{c} d\mathbf{u}_{p+1}^{\nu} \\ d\mathbf{u}_{p+1}^{\nu^{(k)}} \end{array} \right] \tag{31}$$

Important step of the demonstration: We must be aware that for every call into the loop over $p+1$, resisting force $\mathbf{F}_{p+1}^{\nu}$ obviously depends on $\mathbf{u}_{p+1}^{\nu}$ (if the displacement is the unknown of subdomain ν), but also on the kinematic variable of the previous step p through $\mathbf{D}_p^{\nu}$ and $\mathbf{B}_p^{\nu}$.

This same concern holds for the internal equilibrium of subdomain ν, which depends on: $\mathbf{u}_{p+1}^{\nu^{(k)}}$ at the current time step $p+1$, but also on $\mathbf{D}_p^{\nu^{(k)}}$, $\mathbf{B}_p^{\nu^{(k)}}$ from the previous step p.

As a reminder, the following time scheme relationships are respected for the degrees of freedom at the interface of the subdomains, as well as for the internal nodes of subdomain ν:

$$\left\{ \begin{array}{l} \mathbf{v}_{p+1}^{\nu} = C^{\nu}\mathbf{u}_{p+1}^{\nu} + \mathbf{D}_p^{\nu} \\ \mathbf{a}_{p+1}^{\nu} = A^{\nu}\mathbf{u}_{p+1}^{\nu} + \mathbf{B}_p^{\nu} \end{array} \right. \quad and \quad \left\{ \begin{array}{l} \mathbf{v}_{p+1}^{\nu^{(k)}} = C^{\nu}\mathbf{u}_{p+1}^{\nu^{(k)}} + \mathbf{D}_p^{\nu^{(k)}} \\ \mathbf{a}_{p+1}^{\nu^{(k)}} = A^{\nu}\mathbf{u}_{p+1}^{\nu^{(k)}} + \mathbf{B}_p^{\nu^{(k)}} \end{array} \right. \tag{32}$$

Let's now consider a new variable $\mathbf{W}$ collecting the kinematics at the previous time step p:

$$\mathbf{W}_p^{\nu} = {}^t \left[\begin{array}{cccc} \mathbf{B}_p^{\nu} & \mathbf{B}_p^{\nu^{(k)}} & \mathbf{D}_p^{\nu} & \mathbf{D}_p^{\nu^{(k)}} \end{array} \right] \tag{33}$$

Note:. In the following section, $\mathbf{W}_{\mathbf{p}}^{\nu}$ will also be written as:

$$\mathbf{W}_{\mathbf{p}}^{\nu} = \left[\begin{array}{c} \mathbf{B}_p^{g\nu} \\ \mathbf{D}_p^{g\nu} \end{array} \right] \tag{34}$$

with $\mathbf{B}_p^{g\nu}$ (expressed with superscript g) because it collects all the degrees of freedom of subdomain ν and can be decomposed into $\mathbf{B}_p^{\nu}$ for the degrees of freedom at the interface and $\mathbf{B}_p^{\nu^{(k)}}$ for the internal degrees of freedom. This same nomenclature holds for $\mathbf{D}_p^{g\nu}$.

Let's recall that:

$$\mathbf{U}_{p+1}^{\nu} = {}^t \left[\begin{array}{cc} \mathbf{u}_{p+1}^{\nu} & \mathbf{u}_{p+1}^{\nu^{(k)}} \end{array} \right] \tag{35}$$

Then, since the global resisting force can be written as:

$$\mathbf{F}_{p+1}^{g\nu} = \mathbf{F}_{p+1}^{g\nu}\left(\mathbf{u}_{p+1}^{\nu}, \mathbf{u}_{p+1}^{\nu^{(k)}}, \mathbf{D}_{p}^{\nu}, \mathbf{B}_{p}^{\nu}, \mathbf{D}_{p}^{\nu^{(k)}}, \mathbf{B}_{p}^{\nu^{(k)}}\right)$$

, we can therefore write the following in more general terms (because subdomain ν is written in displacement):

$$\mathbf{F}_{p+1}^{g\nu} = \mathbf{F}_{p+1}^{g\nu}\left(\mathbf{U}_{p+1}^{\nu}, \mathbf{W}_{p}^{\nu}\right) \tag{36}$$

This expression must now be derived with respect to the domain variable φ (e.g. displacement in the present case):
or:

$$d\mathbf{F}_{p+1}^{g\nu} = \frac{\partial \mathbf{F}_{p+1}^{g\nu}}{\partial \mathbf{U}_{p+1}^{\nu}} d\mathbf{U}_{p+1}^{\nu} + \frac{\partial \mathbf{F}_{p+1}^{g\nu}}{\partial \mathbf{W}_{p}^{\nu}} d\mathbf{W}_{p}^{\nu} \tag{37}$$

This last equation displays two important tangent operator terms:

- $\tilde{\mathbf{K}} = \frac{\partial \mathbf{F}_{p+1}^{g\nu}}{\partial \mathbf{U}_{p+1}^{\nu}}$ is the classical algorithmic tangent operator stemming from the classical assembly in subdomain ν
- $\tilde{\mathbf{S}} = \frac{\partial \mathbf{F}_{p+1}^{g\nu}}{\partial \mathbf{W}_{p}^{\nu}}$ is a complementary term stemming from kinematic variables $\mathbf{W}_{p}^{\nu}$

The multi-time stepping coupling method thus requires, at the level of subdomain ν assembling these two matrices.

4.2.2. Analytical expression of the tangent operators $\tilde{\mathbf{K}}$ *and* $\tilde{\mathbf{S}}$

The linearisation of the global resisting force originating from subdomain ν is expressed as:

$$d\mathbf{F}^{g\nu}\left(\mathbf{U}_{p+1}^{\nu}, \mathbf{V}_{p+1}^{\nu}, \mathbf{A}_{p+1}^{\nu}\right) = \mathbf{M} d\mathbf{A}_{p+1}^{\nu} + \mathbf{C} d\mathbf{V}_{p+1}^{\nu} + \mathbf{K} d\mathbf{U}_{p+1}^{\nu} \tag{38}$$

Note:. As seen above, it is important to note that this linearisation necessarily exists or can in any case can be approximated because it has necessarily been used to obtain the balance of the internal degrees of freedom of subdomain ν,

Lastly, at convergence, Equation 38 is written:

$$\begin{bmatrix} \mathbf{M}_{bb} & \mathbf{M}_{br} \\ \mathbf{M}_{rb} & \mathbf{M}_{rr} \end{bmatrix} \begin{bmatrix} d\mathbf{a}^{\nu}_{p+1} \\ d\mathbf{a}^{\nu^{(k)}}_{p+1} \end{bmatrix} + \begin{bmatrix} \mathbf{C}_{bb} & \mathbf{C}_{br} \\ \mathbf{C}_{rb} & \mathbf{C}_{rr} \end{bmatrix} \begin{bmatrix} d\mathbf{v}^{\nu}_{p+1} \\ d\mathbf{v}^{\nu^{(k)}}_{p+1} \end{bmatrix} + \cdots \tag{39}$$
$$\cdots + \begin{bmatrix} \mathbf{K}_{bb} & \mathbf{K}_{br} \\ \mathbf{K}_{rb} & \mathbf{K}_{rr} \end{bmatrix} \begin{bmatrix} d\mathbf{u}^{\nu}_{p+1} \\ d\mathbf{u}^{\nu^{(k)}}_{p+1} \end{bmatrix} = \begin{bmatrix} d\mathbf{F}^{\nu}_{p+1} \\ 0 \end{bmatrix}$$

Since the time-scheme discretisation is valid into subdomain ν for internal degrees of freedom and dofs at the interface and by differentiating these expressions (knowing that the quantities $\mathbf{B}^{g\nu}_p$ and $\mathbf{D}^{g\nu}_p$ over sub-time steps p are no longer constant, as was the case in single time steps), we obtain (using the notation of Equation 34):

$$\begin{cases} \mathbf{A}^{\nu}_{p+1} = A^{\nu}\mathbf{U}^{\nu}_{p+1} + \mathbf{B}^{g\nu}_p \\ \mathbf{V}^{\nu}_{p+1} = C^{\nu}\mathbf{U}^{\nu}_{p+1} + \mathbf{D}^{g\nu}_p \end{cases} \quad and \quad \begin{cases} d\mathbf{A}^{\nu}_{p+1} = A^{\nu}d\mathbf{U}^{\nu}_{p+1} + d\mathbf{B}^{g\nu}_p \\ d\mathbf{V}^{\nu}_{p+1} = C^{\nu}d\mathbf{U}^{\nu}_{p+1} + d\mathbf{D}^{g\nu}_p \end{cases} \tag{40}$$

Then:

$$d\mathbf{F}^{g\nu}_{p+1} = \left(\mathbf{M}A^{\nu} + \mathbf{C}C^{\nu} + \mathbf{K}\right) d\mathbf{U}^{\nu}_{p+1} + \mathbf{M}d\mathbf{B}^{g\nu}_p + \mathbf{C}d\mathbf{D}^{g\nu}_p \tag{41}$$

And finally:

$$d\mathbf{F}^{g\nu}_{p+1} = \underbrace{\left(\mathbf{M}A^{\nu} + \mathbf{C}C^{\nu} + \mathbf{K}\right)}_{\tilde{\mathbf{K}}} d\mathbf{U}^{\nu}_{p+1} + \underbrace{\begin{bmatrix} \mathbf{M} & \mathbf{C} \end{bmatrix}}_{\tilde{\mathbf{S}}} d\mathbf{W}^{\nu}_p \tag{42}$$

with $\tilde{\mathbf{K}}$ and $\tilde{\mathbf{S}}$ the global algorithmic operators from subdomain ν that contain all the subdomain degrees of freedom (both internal and interface). In practice, $\tilde{\mathbf{S}}$ is as straightforward to assemble as $\tilde{\mathbf{K}}$.

In conclusion, in multi-time stepping, the global tangent operator has two terms and is expressed as:

$$d\mathbf{F}^{g\nu}_{p+1} = \tilde{\mathbf{K}}d\mathbf{U}^{\nu}_{p+1} + \tilde{\mathbf{S}}d\mathbf{W}^{\nu}_p \tag{43}$$

The following section will provide the two-step method to derive the relationship between $d\mathbf{W}^{\nu}_{p+1}$ and $d\mathbf{U}^{\nu}_{p+1}$:

- The first step will show the relationship potentially written for these terms at the subdomain interface (relationship between $d\mathbf{u}^{\nu}_{p+1}$ and $d\mathbf{u}^{\varphi}_{i+1}$);
- Then, the second step will allow for an algorithmic static condensation of the linearised equilibrium equation 43.

4.2.3. Derivation of kinematic variables at the subdomain interface (interface between the subdomains)

In recognition of the continuity in velocities imposed at the interface between the subdomains, this section will be devoted to demonstrating the link between $\mathbf{u}_{p+1}^{\nu}$ and $\mathbf{u}_{i+1}^{\varphi}$.

As regards the time scheme of subdomain ν, the time scheme discretisation equations can be differentiated as follows:

$$\left\{ \begin{array}{l} d\mathbf{u}_{p+1}^{\nu} = C^{\nu^{-1}} \left(d\mathbf{v}_{p+1}^{\nu} - d\mathbf{D}_{p}^{\nu} \right) \\ d\mathbf{a}_{p+1}^{\nu} = A^{\nu} d\mathbf{u}_{p+1}^{\nu} + d\mathbf{B}_{p}^{\nu} \end{array} \right. \tag{44}$$

with:

$$\begin{array}{l} d\mathbf{D}_{p}^{\nu} = -C^{\nu} d\mathbf{u}_{p}^{\nu} + \left(1 - C^{\nu} dt_2\right) d\mathbf{v}_{p}^{\nu} + \left(1 - \frac{1}{2} C^{\nu} dt_2\right) dt_2 d\mathbf{a}_{p}^{\nu} \\ d\mathbf{B}_{p}^{\nu} = -A^{\nu} d\mathbf{u}_{p}^{\nu} - A^{\nu} dt_2 d\mathbf{v}_{p}^{\nu} - A^{\nu} \left(\frac{1}{2} - \frac{1}{A^{\nu} dt_2^2} \right) dt_2^2 d\mathbf{a}_{p}^{\nu} \end{array} \tag{45}$$

These relationships can therefore be written in tensorial form, i.e.:

$$\begin{array}{l} \left[\begin{array}{c} d\mathbf{D}_{p}^{\nu} \\ d\mathbf{B}_{p}^{\nu} \end{array} \right] = \underbrace{\left[\begin{array}{c} -C^{\nu} + \left(1 - C^{\nu} dt_2\right) C^{\nu} + \left(1 - \frac{1}{2} C^{\nu} dt_2\right) dt_2 A^{\nu} \\ -A^{\nu} - A^{\nu} dt_2 C^{\nu} - A^{\nu} \left(\frac{1}{2} - \frac{1}{A^{\nu} dt_2^2} \right) dt_2^2 A^{\nu} \end{array} \right]}_{\mathbf{q}^{\nu}} d\mathbf{u}_{p}^{\nu} + \cdots \\ \cdots \underbrace{\left[\begin{array}{cc} \left(1 - C^{\nu} dt_2\right) & \left(1 - \frac{1}{2} C^{\nu} dt_2\right) dt_2 \\ -A^{\nu} dt_2 & -A^{\nu} \left(\frac{1}{2} - \frac{1}{A^{\nu} dt_2^2} \right) dt_2^2 \end{array} \right]}_{\mathbf{m}^{\nu}} \left[\begin{array}{c} d\mathbf{D}_{p-1}^{\nu} \\ d\mathbf{B}_{p-1}^{\nu} \end{array} \right] \end{array} \tag{46}$$

And finally:

$$\left[\begin{array}{c} d\mathbf{D}_{p}^{\nu} \\ d\mathbf{B}_{p}^{\nu} \end{array} \right] = \mathbf{q}^{\nu} d\mathbf{u}_{p}^{\nu} + \mathbf{m}^{\nu} \left[\begin{array}{c} d\mathbf{D}_{p-1}^{\nu} \\ d\mathbf{B}_{p-1}^{\nu} \end{array} \right] \tag{47}$$

This latter equation is actually a recurrent sequence over p. Matrices $\mathbf{q}^{\nu}$ and $\mathbf{m}^{\nu}$ are new operators that solely depend on time scheme parameters.

The differential in displacement is thus expressed as follows:

$$d\mathbf{u}_{p+1}^{\nu} = \underbrace{\left[\begin{array}{cc} -C^{\nu^{-1}} & 0 \end{array} \right]}_{{}^{t}\mathbf{r}_{u}^{\nu}} \left[\begin{array}{c} d\mathbf{D}_{p}^{\nu} \\ d\mathbf{B}_{p}^{\nu} \end{array} \right] + C^{\nu^{-1}} d\mathbf{v}_{p+1}^{\nu} \tag{48}$$

Next, by replacing the increment of velocity at the interface and since $d\mathbf{v}_{p+1}^{\nu} = d\mathbf{v}_{p+1}^{\varphi} = \lambda_{p+1} d\mathbf{u}_{i+1}^{\varphi} + \lambda_{p} d\mathbf{u}_{i}^{\varphi}$ where $\mathbf{u}_{i}^{\varphi}$ is constant, then: $d\mathbf{v}_{p+1}^{\nu} = \lambda_{p+1} C^{\varphi} d\mathbf{u}_{i+1}^{\varphi}$, it gives:

$$d\mathbf{u}_{p+1}^{\nu} = {}^{t}\mathbf{r}_{u}^{\nu}\left(\mathbf{q}^{\nu}d\mathbf{u}_{p}^{\nu} + \mathbf{m}^{\nu}\left[\begin{array}{c} d\mathbf{D}_{p-1}^{\nu} \\ d\mathbf{B}_{p-1}^{\nu} \end{array}\right]\right) + C^{\nu^{-1}}\lambda_{p+1}C^{\varphi}d\mathbf{u}_{i+1}^{\varphi} \tag{49}$$

Note:. The acceleration can also be deduced, if needed, as:

$$d\mathbf{a}_{p+1}^{\nu} = \underbrace{\left[\begin{array}{cc} -A^{\nu}C^{\nu^{-1}} & 1 \end{array}\right]}_{{}^{t}\mathbf{r}_{a}^{\nu}}\left[\begin{array}{c} d\mathbf{D}_{p}^{\nu} \\ d\mathbf{B}_{p}^{\nu} \end{array}\right] + A^{\nu}C^{\nu^{-1}}d\mathbf{v}_{p+1}^{\nu} \tag{50}$$

Also, the displacement increment is given by:

$$d\mathbf{u}_{p+1}^{\nu} = {}^{t}\mathbf{r}_{u}^{\nu}\mathbf{q}^{\nu}d\mathbf{u}_{p}^{\nu} + {}^{t}\mathbf{r}_{u}^{\nu}\mathbf{m}^{\nu}\mathbf{q}^{\nu}d\mathbf{u}_{p-1}^{\nu} + {}^{t}\mathbf{r}_{u}^{\nu}\mathbf{m}^{\nu}\mathbf{m}^{\nu}\mathbf{q}^{\nu}d\mathbf{u}_{p-2}^{\nu} + \cdots + C^{\nu^{-1}}\lambda_{p+1}C^{\varphi}d\mathbf{u}_{i+1}^{\varphi} \tag{51}$$

Then:

$$d\mathbf{u}_{p+1}^{\nu} = C^{\nu^{-1}}\lambda_{p+1}C^{\varphi}d\mathbf{u}_{i+1}^{\varphi} + \sum_{j=0}^{p} {}^{t}\mathbf{r}_{u}^{\nu}\mathbf{m}^{\nu^{j}}\mathbf{q}^{\nu}d\mathbf{u}_{p-j}^{\nu} \tag{52}$$

Let's now introduce the operator $H_{p+1}^{\nu} = \frac{d\mathbf{u}_{p+1}^{\nu}}{d\mathbf{u}_{i+1}^{\varphi}}$; dividing this equation by $d\mathbf{u}_{i+1}^{\varphi}$ leads to:

$$d\mathbf{u}_{p+1}^{\nu} = H_{p+1}^{\nu}d\mathbf{u}_{i+1}^{\varphi} \tag{53}$$

with:

$$H_{p+1}^{\nu} = C^{\nu^{-1}}\lambda_{p+1}C^{\varphi} + \sum_{j=0}^{p} {}^{t}\mathbf{r}_{u}^{\nu}\mathbf{m}^{\nu^{j}}\mathbf{q}^{\nu}H_{p-j}^{\nu} \tag{54}$$

Note:. If the sub-time step dt_2 is given by $dt_2 = \frac{dt_1}{m}$, then the index p will vary between $p = 0$ and $p + 1 = m$. Moreover, the initial condition on H_{p+1}^{ν} for $p = 0$ is: $H_0^{\nu} = 0$

4.2.4. Algorithmic static condensation to derive the tangent operator stemming from subdomain 2

This section is devoted to showing how the algorithmic tangent operator can be calculated for multi-time stepping in using a static condensation technique.

Important preliminary note:. Until now, the notation of the term $d\mathbf{W}_p^\nu$ had been ordered as follows:

$$d\mathbf{W}_p^\nu = {}^t\left[\begin{array}{cccc} d\mathbf{B}_p^\nu & d\mathbf{B}_p^{\nu(k)} & d\mathbf{D}_p^\nu & d\mathbf{D}_p^{\nu(k)} \end{array}\right] \tag{55}$$

This order was chosen because it was straightforward to demonstrate the form of the additional matrix $\tilde{\mathbf{S}}$.

In order to simplify this demonstration, the following notation for $d\mathbf{W}_p^\nu$ will be used:

$$d\mathbf{W}_p^\nu = \left[\begin{array}{c} d\mathbf{w}_p^\nu \\ d\mathbf{w}_p^{\nu(k)} \end{array}\right] = \left[\begin{array}{c} d\mathbf{D}_p^\nu \\ d\mathbf{B}_p^\nu \\ d\mathbf{D}_p^{\nu(k)} \\ d\mathbf{B}_p^{\nu(k)} \end{array}\right] \tag{56}$$

As a result, a rearrangement of the degrees of freedom of matrix $\tilde{\mathbf{S}}$ is needed. But this rearrangement can be easily handled numerically since such is typically the case when rearranging the common degrees of freedom of the $\tilde{\mathbf{K}}$ matrix.

Next, in using the demonstration from the previous section, which was validated not only for the degrees of freedom at the subdomain interface but also for the internal degrees of freedom of subdomain ν, we obtain:

$$\left[\begin{array}{c} d\mathbf{D}_p^\nu \\ d\mathbf{B}_p^\nu \\ d\mathbf{D}_p^{\nu(k)} \\ d\mathbf{B}_p^{\nu(k)} \end{array}\right] = \underbrace{\left[\begin{array}{cc|cc} & & 0 & 0 \\ & \mathbf{m}^\nu & 0 & 0 \\ \hline 0 & 0 & & \\ 0 & 0 & & \mathbf{m}^\nu \end{array}\right]}_{\mathbf{M}^\nu} \left[\begin{array}{c} d\mathbf{D}_{p-1}^\nu \\ d\mathbf{B}_{p-1}^\nu \\ d\mathbf{D}_{p-1}^{\nu(k)} \\ d\mathbf{B}_{p-1}^{\nu(k)} \end{array}\right] + \underbrace{\left[\begin{array}{cc} & 0 \\ \mathbf{q}^\nu & 0 \\ \hline 0 & \\ 0 & \mathbf{q}^\nu \end{array}\right]}_{\mathbf{Q}^\nu} \left[\begin{array}{c} d\mathbf{u}_p^\nu \\ d\mathbf{u}_p^{\nu(k)} \end{array}\right] \tag{57}$$

which can be easily written in the following form using two new operators $\mathbf{M}^\nu$ and $\mathbf{Q}^\nu$, which are solely dependent on the time scheme in subdomain ν:

$$d\mathbf{W}_p^\nu = \mathbf{M}^\nu d\mathbf{W}_{p-1}^\nu + \mathbf{Q}^\nu d\mathbf{U}_p^\nu \tag{58}$$

Lastly, the expression for the differentiation of the global resisting force of subdomain ν yields the following recurring relationship:

$$d\mathbf{F}_{p+1}^{g\nu} = \tilde{\mathbf{K}} d\mathbf{U}_{p+1}^\nu + \tilde{\mathbf{S}} d\mathbf{W}_p^\nu \tag{59}$$

which can also be written as:

$$\begin{array}{ll} & d\mathbf{F}^{g\nu}_{p+1} = \tilde{\mathbf{K}} d\mathbf{U}^{\nu}_{p+1} + \tilde{\mathbf{S}}\left[\mathbf{M}^{\nu} d\mathbf{W}^{\nu}_{p-1} + \mathbf{Q}^{\nu} d\mathbf{U}^{\nu}_{p}\right] \\ \Leftrightarrow & d\mathbf{F}^{\mathbf{g}\nu}_{p+1} = \tilde{\mathbf{K}} d\mathbf{U}^{\nu}_{p+1} + \tilde{\mathbf{S}}\left[\mathbf{M}^{\nu}\left[\mathbf{M}^{\nu} d\mathbf{W}^{\nu}_{p-2} + \mathbf{Q}^{\nu} d\mathbf{U}^{\nu}_{p-1}\right] + \mathbf{Q}^{\nu} d\mathbf{U}^{\nu}_{p}\right] \end{array} \tag{60}$$

Then:

$$d\mathbf{F}^{g\nu}_{p+1} = \tilde{\mathbf{K}} d\mathbf{U}^{\nu}_{p+1} + \tilde{\mathbf{S}}\mathbf{Q}^{\nu} d\mathbf{U}^{\nu}_{p} + \tilde{\mathbf{S}}\mathbf{M}^{\nu}\mathbf{Q}^{\nu} d\mathbf{U}_{p-1} + \tilde{\mathbf{S}}\mathbf{M}^{\nu}\mathbf{M}^{\nu}\mathbf{Q}^{\nu} d\mathbf{U}_{p-2} + \cdots \tag{61}$$

Ultimately:

$$d\mathbf{F}^{g\nu}_{p+1} = \tilde{\mathbf{K}} d\mathbf{U}^{\nu}_{p+1} + \sum_{j=0}^{p} \tilde{\mathbf{S}}\mathbf{M}^{\nu^j}\mathbf{Q}^{\nu} d\mathbf{U}^{\nu}_{p-j} \tag{62}$$

The term $d\mathbf{U}^{\nu}_{p+1}$ can be expressed using the $\mathbf{H}^{\nu}_{p+1}$ matrix. On the other hand, the $d\mathbf{u}^{\nu^{(k)}}_{p+1}$ term (internal to subdomain ν) will be deduced in the next subsection from the algorithmic static condensation of this operator.

Algorithmic static condensation. The algorithmic static condensation is performed on the internal equilibrium equation, which vanishes at convergence.

$$\mathbf{F}^{g\nu}_{p+1} = \begin{bmatrix} \mathbf{F}^{\nu}_{p+1} \\ -\mathbf{R}^{(k)}_{p+1} \end{bmatrix} = \underbrace{\begin{bmatrix} \mathbf{F}^{\nu}_{p+1} \\ \mathbf{0} \end{bmatrix}}_{at\ \ convergence} \quad then \quad d\mathbf{F}^{g\nu}_{p+1} = \begin{bmatrix} d\mathbf{F}^{\nu}_{p+1} \\ \mathbf{0} \end{bmatrix} \tag{63}$$

The 2nd equation (equal to $\mathbf{0}$) can be written in blocks (on the internal degrees of freedom of subdomain ν):

$$\tilde{\mathbf{K}}_{rb} d\mathbf{u}^{\nu}_{p+1} + \tilde{\mathbf{K}}_{rr} d\mathbf{u}^{\nu^{(k)}}_{p+1} + \sum_{j=0}^{p} \left[\left(\tilde{\mathbf{S}}\mathbf{M}^{\nu^j}\mathbf{Q}^{\nu}\right)_{rb} d\mathbf{u}^{\nu}_{p-j} + \left(\tilde{\mathbf{S}}\mathbf{M}^{\nu^j}\mathbf{Q}^{\nu}\right)_{rr} d\mathbf{u}^{\nu^{(k)}}_{p-j}\right] = \mathbf{0} \tag{64}$$

The resolution of this equation allows calculating the relationship between the internal degrees of freedom $d\mathbf{u}^{\nu^{(k)}}_{p-j}$ and the displacements at the interface of subdomain ν: $d\mathbf{u}^{\nu}_{p+1} = H^{\nu}_{p+1} d\mathbf{u}^{\varphi}_{i+1}$.

$$d\mathbf{u}_{p+1}^{\nu^{(k)}} = -\tilde{\mathbf{K}}_{rr}^{-1}\left[\tilde{\mathbf{K}}_{rb}H_{p+1}^{\nu}d\mathbf{u}_{i+1}^{\varphi} + \sum_{j=0}^{p}\left[\left(\tilde{\mathbf{S}}\mathbf{M}^{\nu^j}\mathbf{Q}^{\nu}\right)_{rb}H_{p-j}^{\nu}d\mathbf{u}_{i+1}^{\varphi} + \left(\tilde{\mathbf{S}}\mathbf{M}^{\nu^j}\mathbf{Q}^{\nu}\right)_{rr}d\mathbf{u}_{p-j}^{\nu^{(k)}}\right]\right] \tag{65}$$

Let's now consider, for the internal degrees of freedom, an operator $\mathbf{T}_{p-j}$ such that: $d\mathbf{u}_{p-j}^{\nu^{(k)}} = \mathbf{T}_{p-j}d\mathbf{u}_{i+1}^{\varphi}$

The previous equation can then be written as:

$$d\mathbf{u}_{p+1}^{\nu^{(k)}} = \underbrace{-\tilde{\mathbf{K}}_{rr}^{-1}\left[\tilde{\mathbf{K}}_{rb}H_{p+1}^{\nu} + \sum_{j=0}^{p}\left[\left(\tilde{\mathbf{S}}\mathbf{M}^{\nu^j}\mathbf{Q}^{\nu}\right)_{rb}H_{p-j}^{\nu} + \left(\tilde{\mathbf{S}}\mathbf{M}^{\nu^j}\mathbf{Q}^{\nu}\right)_{rr}\mathbf{T}_{p-j}\right]\right]}_{\mathbf{T}_{p+1}}d\mathbf{u}_{i+1}^{\varphi} \tag{66}$$

The operator $\mathbf{T}_{p+1}$ able to be calculated by a recurrent sequence allows condensing the internal degrees of freedom of subdomain ν on the degrees of freedom at the interface of subdomain: $d\mathbf{u}_{p+1}^{\nu^{(k)}} = \mathbf{T}_{p+1}d\mathbf{u}_{i+1}^{\varphi}$

Next, by introducing into the first equation of the system in 63, we obtain:

$$\tilde{\mathbf{K}}_{bb}d\mathbf{u}_{p+1}^{\nu} + \tilde{\mathbf{K}}_{br}d\mathbf{u}_{p+1}^{\nu^{(k)}} + \sum_{j=0}^{p}\left[\left(\tilde{\mathbf{S}}\mathbf{M}^{\nu^j}\mathbf{Q}^{\nu}\right)_{bb}d\mathbf{u}_{p-j}^{\nu} + \left(\tilde{\mathbf{S}}\mathbf{M}^{\nu^j}\mathbf{Q}^{\nu}\right)_{br}d\mathbf{u}_{p-j}^{\nu^{(k)}}\right] = d\mathbf{F}_{p+1}^{\nu} \tag{67}$$

then:

$$\left[\tilde{\mathbf{K}}_{bb}H_{p+1}^{\nu} + \tilde{\mathbf{K}}_{br}\mathbf{T}_{p+1} + \sum_{j=0}^{p}\left[\left(\tilde{\mathbf{S}}\mathbf{M}^{\nu^j}\mathbf{Q}^{\nu}\right)_{bb}H_{p-j}^{\nu} + \left(\tilde{\mathbf{S}}\mathbf{M}^{\nu^j}\mathbf{Q}^{\nu}\right)_{br}\mathbf{T}_{p-j}\right]\right]d\mathbf{u}_{i+1}^{\varphi} = d\mathbf{F}_{p+1}^{\nu} \tag{68}$$

and finally the algorithmic tangent operator is equal to:

$$\frac{\partial \mathbf{F}_{p+1}^{\nu}}{\partial \mathbf{u}_{i+1}^{\varphi}} = \underbrace{\tilde{\mathbf{K}}_{bb}H_{p+1}^{\nu} + \tilde{\mathbf{K}}_{br}\mathbf{T}_{p+1} + \sum_{j=0}^{p}\left[\left(\tilde{\mathbf{S}}\mathbf{M}^{\nu^j}\mathbf{Q}^{\nu}\right)_{bb}H_{p-j}^{\nu} + \left(\tilde{\mathbf{S}}\mathbf{M}^{\nu^j}\mathbf{Q}^{\nu}\right)_{br}\mathbf{T}_{p-j}\right]}_{\tilde{\mathbf{k}}_{p+1}} \tag{69}$$

In practice therefore, the algorithmic tangent operator is calculated on a

recurring sequence as follows:

$$\begin{cases} H_{p+1}^{\nu} = C^{\nu^{-1}} \lambda_{p+1} C^{\varphi} + \sum_{j=0}^{p} {}^{t}\mathbf{r}_u^{\nu} \mathbf{m}^{\nu^j} \mathbf{q}^{\nu} H_{p-j}^{\nu} \\ \mathbf{T}_{p+1} = -\tilde{\mathbf{K}}_{rr}^{-1} \left[\tilde{\mathbf{K}}_{rb} H_{p+1}^{\nu} + \sum_{j=0}^{p} \left[\left(\tilde{\mathbf{S}}\mathbf{M}^{\nu^j} \mathbf{Q}^{\nu} \right)_{rb} H_{p-j}^{\nu} + \left(\tilde{\mathbf{S}}\mathbf{M}^{\nu^j} \mathbf{Q}^{\nu} \right)_{rr} \mathbf{T}_{p-j} \right] \right] \\ \tilde{\mathbf{k}}_{p+1} = \tilde{\mathbf{K}}_{bb} H_{p+1}^{\nu} + \tilde{\mathbf{K}}_{br} \mathbf{T}_{p+1} + \sum_{j=0}^{p} \left[\left(\tilde{\mathbf{S}}\mathbf{M}^{\nu^j} \mathbf{Q}^{\nu} \right)_{bb} H_{p-j}^{\nu} + \left(\tilde{\mathbf{S}}\mathbf{M}^{\nu^j} \mathbf{Q}^{\nu} \right)_{br} \mathbf{T}_{p-j} \right] \end{cases} \tag{70}$$

Note:. When the time step is not subdivided, the classical static condensation is found naturally by simplifying this expression (since index j extends from $j = 0$ to 0 with $H_0^{\nu} = 0$):

Then: $H_1^{\nu} = C^{\nu^{-1}} C^{\varphi}$ and $\mathbf{T}_1 = -\tilde{\mathbf{K}}_{rr}^{-1} \left[\tilde{\mathbf{K}}_{rb} C^{\nu^{-1}} C^{\varphi} \right]$

And lastly: $\tilde{\mathbf{k}}_1 = \left(\tilde{\mathbf{K}}_{bb} - \tilde{\mathbf{K}}_{br} \tilde{\mathbf{K}}_{rr}^{-1} \tilde{\mathbf{K}}_{rb} \right) C^{\nu^{-1}} C^{\varphi}$, which corresponds naturally to the classical static condensation obtained in Equation 24.

The details of the this implementation are given below in algorithm 5.1.

5. Time scheme coupling from second-order Newmark to first-order Euler+θ time schemes

5.1. Motivations

It may be very worthwhile to keep the Newmark time scheme for dynamic structure models in order to take advantage of the damping characteristics of the time scheme. However, a non-smooth dynamic Euler+θ time scheme is better suited to treat impacts since Euler's θ scheme is of the first order and can efficiently handle impact-related velocity discontinuities using linear complementary problems (LCP) Acary (2013).

Consequently, the coupling of a Newmark time scheme with internal subdomains treated with Euler+θ can be very attractive and thus open up fairly simple paths for dealing with structural and non-smooth dynamics and impact applications (e.g. falling blocks, building pounding).

The special numerical features in this coupling, compared to Newmark-to-Newmark, are as follows:

- writing of the displacements and velocities at $i+\theta$ in Euler+θ time schemes will require a 2nd operation for transfer of the kinematics variables from subdomain φ to subdomain ν;
- the quantity returned by Euler+θ is a pulse (at $i+\theta$) that will need to be modified into a resisting force (and at time step $i+1$)
- the velocity, as the kinematic unknown variable in the Euler+θ method; if boundary continuity of the domains formulated in velocity can be assumed, then this would simplify the calculation of the tangent operator in multi-time stepping algorithms since the time connection with subdomain φ will be much simpler.

5.2. Synchronous coupling (same time steps in both time schemes)

The displacements and velocities of subdomain ν can be expressed as follows (valid for internal degrees of freedom and dofs at the interface) from Euler+θ time scheme:

$$\left\{ \begin{array}{l} \mathbf{u}_{i+1}^{\nu} = \mathbf{u}_{i}^{\nu} + dt_2 \mathbf{v}_{i+\theta}^{\nu} \\ \mathbf{v}_{i+\theta}^{\nu} = (1-\theta^{\nu}) \mathbf{v}_{i}^{\nu} + \theta^{\nu} \mathbf{v}_{i+1}^{\nu} \\ \mathbf{u}_{i+\theta}^{\nu} = (1-\theta^{\nu}) \mathbf{u}_{i}^{\nu} + \theta^{\nu} \mathbf{u}_{i+1}^{\nu} \end{array} \right. \tag{71}$$

This expression can be written in a more general form as:

$$\left\{ \begin{array}{l} \mathbf{v}_{i+1}^{\nu} = C^{\nu} \mathbf{u}_{i+1}^{\nu} + \mathbf{D}_{i}^{\nu} \\ \mathbf{a}_{i+1}^{\nu} = NA \end{array} \right. \tag{72}$$

with:

$$\left\{ \begin{array}{l} C^{\nu} = \frac{1}{\theta^{\nu} dt_2} \\ \mathbf{D}_{i}^{\nu} = -\frac{1}{\theta^{\nu} dt_2} \left(\mathbf{u}_{i}^{\nu} + dt_2 \left(1-\theta^{\nu}\right) \mathbf{v}_{i}^{\nu} \right) \end{array} \right. \tag{73}$$

This expression is not directly useful because the internal resolution of subdomain ν needs to be expressed with displacements and velocities at $i+\theta$, both of which are functions of the velocity at time step $i+1$.

The following relationships are then need to be employed inside the subdomain ν:

$$\left\{ \begin{array}{l} \mathbf{u}_{i+\theta}^{\nu} = \alpha^{\nu} \mathbf{v}_{i+1}^{\nu} + \beta_{i}^{\nu} \\ \mathbf{v}_{i+\theta}^{\nu} = \theta^{\nu} \mathbf{v}_{i+1}^{\nu} + \left(1-\theta^{\nu}\right) \mathbf{v}_{i}^{\nu} \end{array} \right. \quad with: \quad \left\{ \begin{array}{l} \alpha^{\nu} = {\theta^{\nu}}^2 dt_2 \\ \beta_{i}^{\nu} = -dt_2 \left(1-\theta^{\nu}\right)^2 \mathbf{v}_{i}^{\nu} - \theta^{\nu} dt_2 \mathbf{D}_{i}^{\nu} \end{array} \right. \tag{74}$$

Everything depends on the velocity at time step $i+1$ (since it is the typical unknown in the Euler+θ time scheme). This quantity will then be directly correlated with the kinematic variables of subdomain φ (which may be displacement, velocity or acceleration and necessitate use of the time coupling equation).

5.2.1. Resisting force at the interface between the subdomains

Application of the VPP* projected onto the velocity field (since it is the field imposing continuity at interface $\mathbf{v}_{i+1}^{\varphi^*} = \mathbf{v}_{i+1}^{\nu^*}$) gives:

$$\forall \mathbf{v}^*,\ {}^t\mathbf{v}_{i+1}^{\varphi^*}\mathbf{F}_{i+1}^{\varphi}\left(\mathbf{u}_{i+1}^{\varphi}, \mathbf{v}_{i+1}^{\varphi}, \mathbf{a}_{i+1}^{\varphi}\right) + {}^t\mathbf{v}_{i+1}^{\nu^*}\mathbf{F}_{i+1}^{\nu}\left(\mathbf{u}_{i+\theta}^{\nu}, \mathbf{v}_{i+\theta}^{\nu}, \mathbf{v}_{i+1}^{\nu}\right) = 0 \quad (75)$$

The difficulty here stems from the fact that subdomain ν returns a pulse at the time step $i+\theta$ (pulse $\mathbf{P}_{i+\theta}^{\nu}$) and not directly the resisting force at time step $i+1$. Another transformation is then needed.

From the definition of the Euler+θ time scheme, the pulse at $i+\theta$ can be calculated as follows:

The resisting force equilibrium is then:

$$\forall \mathbf{v}^*,\ {}^t\mathbf{v}_{i+1}^{\varphi^*}\mathbf{F}_{i+1}^{\varphi} + {}^t\mathbf{v}_{i+1}^{\nu^*}\frac{1}{\theta^{\nu}dt^{\nu}}\left[\mathbf{P}_{i+\theta}^{\nu} - (1-\theta^{\nu})\,\mathbf{P}_{i}^{\nu}\right] = 0 \quad (76)$$

which can be written using a time scheme coefficient:

$$\forall \mathbf{v}^*,\ {}^t\mathbf{v}_{i+1}^{\varphi^*}\mathbf{F}_{i+1}^{\varphi} + {}^t\mathbf{v}_{i+1}^{\nu^*}\underbrace{C^{\nu}\left[\mathbf{P}_{i+\theta}^{\nu} - (1-\theta^{\nu})\,\mathbf{P}_{i}^{\nu}\right]}_{\mathbf{F}_{i+1}^{\nu}} = 0 \quad (77)$$

Given the velocity continuity at interface ($\mathbf{v}_{i+1}^{\varphi^*} = \mathbf{v}_{i+1}^{\nu^*}$), the resisting force does not require any further modification from subdomain ν to subdomain φ; hence, the resisting force is:

$$\mathbf{F}_{i+1}^{\nu} = C^{\nu}\left[\mathbf{P}_{i+\theta}^{\nu} - (1-\theta^{\nu})\,\mathbf{P}_{i}^{\nu}\right] \quad (78)$$

Note:. We must be careful in the case of nonzero initial conditions at the interface and for the internal degrees of freedom of subdomain ν, because the initial pulse must be calculated with care. Indeed, if this initial pulse is miscalculated, subdomain ν could be led on a wrong kinematic trajectory.

5.2.2. Algorithmic tangent operator

In order to maintain quadratic convergence of subdomain φ, subdomain ν must return the $\frac{\partial \mathbf{F}^{\nu}_{i+1}}{\partial \mathbf{u}^{\varphi}_{i+1}}$ operator.

In the case of the same time-stepping in the both subdomains, all that had been calculated during the previous step is to remain constant, thus $\frac{\partial \mathbf{P}^{\nu}_{i}}{\partial \mathbf{u}^{\varphi}_{i+1}} = \mathbf{0}$

A final step requires calculating $\frac{\partial \mathbf{F}^{\nu}_{i+1}}{\partial \mathbf{u}^{\varphi}_{i+1}} = C^{\nu} \frac{\partial \mathbf{P}^{\nu}_{i+\theta}}{\partial \mathbf{u}^{\varphi}_{i+1}}$

Let's note that $\mathbf{v}^{\varphi}_{i+1} = \mathbf{v}^{\nu}_{i+1}$; a quick demonstration of the evaluation of this term can be performed as follows:

$$\frac{\partial \mathbf{F}^{\nu}_{i+1}}{\partial \mathbf{u}^{\varphi}_{i+1}} = C^{\nu} \frac{\partial \mathbf{P}^{\nu}_{i+\theta}}{\partial \mathbf{v}^{\nu}_{i+1}} \frac{\partial \mathbf{v}^{\nu}_{i+1}}{\partial \mathbf{u}^{\varphi}_{i+1}} = C^{\nu} \underbrace{\frac{\partial \mathbf{P}^{\nu}_{i+\theta}}{\partial \mathbf{v}^{\nu}_{i+1}}}_{\tilde{\mathbf{m}}} \underbrace{\frac{\partial \mathbf{v}^{\varphi}_{i+1}}{\partial \mathbf{u}^{\varphi}_{i+1}}}_{C^{\varphi}\mathbf{I}_{rr}} = C^{\varphi} C^{\nu} \tilde{\mathbf{m}} \tag{79}$$

with $\tilde{\mathbf{m}}$ being the condensed operator returned by subdomain ν (which is used in any event in its internal resolution).

5.3. Coupling the 2 subdomains with multi-time stepping

5.3.1. Resisting forces at the interface between subdomains

The resisting force must be provided to the Newmark time scheme (subdomain φ at last time step $p+1 = m$). Thus, the impulse given in $p+\theta$ must be then calculated at the last time sub-step $p+1$ to give the force at $i+1$:

$$\mathbf{F}^{\nu}_{i+1} = C^{\nu} \left[\mathbf{P}^{\nu}_{p+\theta} - (1-\theta^{\nu}) \mathbf{P}^{\nu}_{p} \right] \tag{80}$$

5.3.2. Algorithmic static condensation to get the tangent operator

In multi-time stepping, the derivatives of the kinematic terms of the previous time step p must be taken into account.

As has been demonstrated for the Newmark/Newmark coupling, the variation of the equilibrium equation then yields:

$$d\mathbf{P}^{g\nu}_{p+\theta} = \underbrace{\left[\mathbf{M} + dt_2 \mathbf{C}\theta^{\nu} + dt_2 \mathbf{K}\alpha^{\nu}\right]}_{\tilde{\mathbf{M}}} d\mathbf{V}^{\nu}_{p+1} + \ldots \tag{81}$$

$$\ldots + \underbrace{\left[\; -\mathbf{M} + dt_2 \mathbf{C}\left(1-\theta^{\nu}\right) - dt_2 \mathbf{K} dt_2 \left(1-\theta^{\nu}\right)^2 , \quad -dt_2 \mathbf{K} C^{\nu^{-1}} \; \right]}_{\tilde{\mathbf{S}}} \underbrace{\begin{bmatrix} d\mathbf{V}^{\nu}_{p} \\ d\mathbf{D}^{g\nu}_{p} \end{bmatrix}}_{d\mathbf{W}^{\nu}_{p}}$$

where $\mathbf{D}_p^{g\nu}$ is the array collecting all of subdomain ν degrees of freedom (both internal and at the interface with subdomain φ), such that: $\mathbf{D}_p^{g\nu} = {}^t\begin{bmatrix} \mathbf{D}_p^{\nu} & \mathbf{D}_p^{\nu^{(k)}} \end{bmatrix}$

Finally:

$$d\mathbf{P}_{p+\theta}^{g\nu} = \tilde{\mathbf{M}} d\mathbf{V}_{p+1}^{\nu} + \tilde{\mathbf{S}} d\mathbf{W}_p^{\nu} \tag{82}$$

At this point, the kinematics of the previous time steps must be calculated and linked with those at the interface with subdomain φ in the aim of performing the algorithmic static condensation of this system. As opposed to the previous Newmark case, where the main unknown was displacement, the unknown here is velocity and thus explicitly linked at each time step to the velocity imposed by the coupling at the interface.

Hence:

$$\mathbf{v}_{p+1}^{\nu} = \lambda_{p+1}\mathbf{v}_{i+1}^{\varphi} + \lambda_p \mathbf{v}_i^{\varphi} \quad then \quad d\mathbf{v}_{p+1}^{\nu} = \underbrace{\lambda_{p+1} C^{\varphi}}_{H_{p+1}^{\nu}} d\mathbf{u}_{i+1}^{\varphi} \tag{83}$$

Next, $d\mathbf{W}_p^{\nu}$ can be calculated at each sub-time step using a recurrent sequence and velocity $d\mathbf{V}_{p+1}^{\nu}$ as follows. The expression can ultimately be expressed as a function of all velocities computed at all time steps p, which is the unknown velocity in subdomain ν.

Indeed, let's recall that:

$$\mathbf{D}_p^{\nu} = -C^{\nu}\left(\mathbf{u}_p^{\nu} + dt_2\left(1-\theta^{\nu}\right)\mathbf{v}_p^{\nu}\right) \quad with \quad \mathbf{u}_{p+1}^{\nu} = C^{\nu^{-1}}\left(\mathbf{v}_{p+1}^{\nu} - \mathbf{D}_p^{\nu}\right) \tag{84}$$

A recurrence sequence can then be introduced on $\mathbf{D}_p^{\nu}$. This sequence may be expressed as a function of the velocities (given that it is the main unknown of subdomain ν):

$$\mathbf{D}_p^{\nu} = -\left(1 + C^{\nu} dt_2\left(1-\theta^{\nu}\right)\right)\mathbf{v}_p^{\nu} + \mathbf{D}_{p-1}^{\nu} \tag{85}$$

which can be expressed in the tensorial form as follows:

$$\begin{bmatrix} \mathbf{v}_p^{\nu} \\ \mathbf{D}_p^{\nu} \end{bmatrix} = \underbrace{\begin{bmatrix} 1 \\ -\left[1 + C^{\nu} dt_2\left(1-\theta^{\nu}\right)\right] \end{bmatrix}}_{\mathbf{q}^{\nu}} \mathbf{v}_p^{\nu} + \underbrace{\begin{bmatrix} 0 & 0 \\ 0 & 1 \end{bmatrix}}_{\mathbf{m}^{\nu}} \underbrace{\begin{bmatrix} \mathbf{v}_{p-1}^{\nu} \\ \mathbf{D}_{p-1}^{\nu} \end{bmatrix}}_{\mathbf{w}_{p-1}^{b\nu}} \tag{86}$$

This leads to the following expression:

$$\mathbf{w}_p^{b\nu} = \mathbf{q}^\nu \mathbf{v}_p^\nu + \mathbf{m}^\nu \mathbf{w}_{p-1}^{b\nu} \tag{87}$$

To facilitate its construction, the $d\mathbf{W}_p^\nu$ vector is rearranged (which simply requires rearranging the columns of the $\tilde{\mathbf{S}}$ matrix):

$$d\mathbf{W}_p^\nu = \begin{bmatrix} d\mathbf{w}_p^{b\nu} \\ d\mathbf{w}_p^{r\nu} \end{bmatrix} = \begin{bmatrix} d\mathbf{v}_p^\nu \\ d\mathbf{D}_p^\nu \\ d\mathbf{v}_p^{\nu^{(k)}} \\ d\mathbf{D}_p^{\nu^{(k)}} \end{bmatrix} = \underbrace{\begin{bmatrix} \mathbf{m}^\nu & 0 & 0 \\ 0 & 0 & 0 \\ 0 & 0 & \mathbf{m}^\nu \end{bmatrix}}_{\mathbf{M}^\nu} \begin{bmatrix} d\mathbf{v}_{p-1}^\nu \\ d\mathbf{D}_{p-1}^\nu \\ d\mathbf{v}_{p-1}^{\nu^{(k)}} \\ d\mathbf{D}_{p-1}^{\nu^{(k)}} \end{bmatrix} + \underbrace{\begin{bmatrix} \mathbf{q}^\nu & 0 \\ 0 & 0 \\ 0 & \mathbf{q}^\nu \end{bmatrix}}_{\mathbf{Q}^\nu} \begin{bmatrix} d\mathbf{v}_p^\nu \\ d\mathbf{v}_p^{\nu^{(k)}} \end{bmatrix} \tag{88}$$

Finally, as in the case of Equation 62 in the Newmark-to-Newmark coupling, the differentiation of the equilibrium equation here (from subdomain ν defined in velocity) therefore provides:

$$d\mathbf{P}_{p+\theta}^{g\nu} = \tilde{\mathbf{M}} d\mathbf{V}_{p+1}^\nu + \sum_{j=0}^{p} \tilde{\mathbf{S}} \mathbf{M}^{\nu^j} \mathbf{Q}^\nu d\mathbf{V}_{p-j}^\nu \tag{89}$$

For every time step p, the second equation is introduced into the first (algorithmic static condensation) as follows:

$$\begin{cases} H_{p+1}^\nu = \lambda_{p+1} C^\varphi \\ \mathbf{T}_{p+1} = -\tilde{\mathbf{M}}_{rr}^{-1} \left[\tilde{\mathbf{M}}_{rb} H_{p+1}^\nu + \sum_{j=0}^{p} \left[\left(\tilde{\mathbf{S}} \mathbf{M}^{\nu^j} \mathbf{Q}^\nu \right)_{rb} H_{p-j}^\nu + \left(\tilde{\mathbf{S}} \mathbf{M}^{\nu^j} \mathbf{Q}^\nu \right)_{rr} \mathbf{T}_{p-j} \right] \right] \\ \tilde{\mathbf{m}}_{p+\theta} = \tilde{\mathbf{M}}_{bb} H_{p+1}^\nu + \tilde{\mathbf{M}}_{br} \mathbf{T}_{p+1} + \sum_{j=0}^{p} \left[\left(\tilde{\mathbf{S}} \mathbf{M}^{\nu^j} \mathbf{Q}^\nu \right)_{bb} H_{p-j}^\nu + \left(\tilde{\mathbf{S}} \mathbf{M}^{\nu^j} \mathbf{Q}^\nu \right)_{br} \mathbf{T}_{p-j} \right] \end{cases} \tag{90}$$

This last equation allows computing the operator $\tilde{\mathbf{m}}_{p+\theta}$, although this operator is actually $\tilde{\mathbf{m}}_{p+\theta} = \frac{\partial \mathbf{P}_{p+\theta}^\nu}{\partial \mathbf{u}_{i+1}^\varphi}$ and originates from a pulse at $p+\theta$.

This operator must then be changed at time step $i+1$ using the relationship $\mathbf{P}_{p+1}^\nu = \frac{1}{\theta^\nu} \left[\mathbf{P}_{p+\theta}^\nu - (1-\theta^\nu) \mathbf{P}_p^\nu \right]$.

Another recurrent sequence is used in order to obtain the algorithmic tangent operator to be used by subdomain φ:

$$\frac{\partial \mathbf{F}^{\nu}_{p+1}}{\partial \mathbf{u}^{\varphi}_{i+1}} = \frac{1}{dt}\frac{\partial \mathbf{P}^{\nu}_{p+1}}{\partial \mathbf{u}^{\varphi}_{i+1}} = C^{\nu}\left[\tilde{\mathbf{m}}_{p+\theta} - (1-\theta^{\nu})\left(\frac{1}{\theta^{\nu}}\left[\tilde{\mathbf{m}}_{p-1+\theta} - (1-\theta^{\nu})\left(\frac{1}{\theta^{\nu}}\left[\tilde{\mathbf{m}}_{p-2+\theta} - (1-\theta^{\nu})\left(\frac{1}{\theta^{\nu}}\left[\ldots\right]\right)\right]\right)\right]\right)\right] \tag{91}$$

Next, the algorithmic tangent operator to be used by subdomain φ within the framework of a resisting force (instead of a pulse) at time step $i+1$:

$$\tilde{\mathbf{m}}_{p+1} = \frac{\partial \mathbf{F}^{\nu}_{p+1}}{\partial \mathbf{u}^{\varphi}_{i+1}} = C^{\nu}\sum_{j=0}^{p}\left[\frac{-(1-\theta^{\nu})}{\theta^{\nu}}\right]^{j}\tilde{\mathbf{m}}_{p-j+\theta} \tag{92}$$

The computation of this tangent operator, even if its mathematical expression seems to be complex, can be easily implemented in the time-stepping algorithm.

Note:. It is clear that for $0 \leq \theta < \frac{1}{2}$ the term $\left(\frac{1-\theta}{\theta}\right)^{j}$ can become very large and even becomes impossible to calculate when $\theta = 0$ (i.e. when the Euler time scheme is explicit). Otherwise, this term is equal to 1 when $\theta = \frac{1}{2}$.

This is the reason why, in using this approach, the Euler+θ method can only be employed when accompanied by the assumption that $\theta \in \left[\frac{1}{2}, 1\right]$.

The implementation details for the various time schemes are given in Algorithm 5.1.

6. Truncation error analysis for a simple 2 degrees-of-freedom system

A two degrees-of-freedom system (also presented in Belytschko et al. (1979)) is considered herein in order to study the accuracy order of the coupling algorithm. Such a system is composed of two subdomains with mass, spring and dashpot (see Fig. 4).

The system parameters for these simulations are: $k_1 = k_2 = 200$, $k_3 = 0$, $c_1 = c_2 = 10$, $c_3 = 0$ and $m_1 = m_3 = 10$. The initial conditions in displacement are: $u_1 = 0.5$ (i.e $u_1^{\varphi} = u^{\nu} = 0.5$) and $u_2 = 1$ (i.e $u^{\nu^{(k)}} = 1$). An analytical solution has been found in order to calculate the errors in displacements, velocities and accelerations.

Three distinct simulations could then be carried out:

- A reference simulation is performed in a global manner using a Newmark time scheme with a time step dt;

Algorithm for the HATI primal approach
(Computation of the algorithmic tangent operator)

(i) ***Require*** time scheme parameters for the various domains
  A_1, C_1, A_2, C_2
  dt_2, θ_2 (according to the time scheme family)
(ii) ***Require*** initial conditions on the time step:
  $\mathbf{u}_i^\varphi$, $\mathbf{v}_i^\varphi$, (and $\mathbf{a}_i^\varphi$) for domain φ
  $\mathbf{u}_i^\nu$, $\mathbf{v}_i^\nu$, (and $\mathbf{a}_i^\nu$) for domain ν
(iii) ***Compute*** $\mathbf{D}_i^\varphi$ (and $\mathbf{B}_i^\varphi$) and $\mathbf{D}_i^\nu$ (and $\mathbf{B}_i^\nu$) according to the time scheme family
(iv) ***Initialise*** the sub-time steps $p=0$: $\mathbf{u}_p^\nu = \mathbf{u}_i^\nu$, $\mathbf{v}_p^\nu = \mathbf{v}_i^\nu$ (and $\mathbf{a}_p^\nu = \mathbf{a}_i^\nu$)
  and initialise the internal variables
(v) ***Compute*** (only once) the condensation operators of subdomain ν : $\mathbf{M}^\nu$ and $\mathbf{Q}^\nu$
(vi) ***For each sub-time step*** $j = 1$ ***to*** $N = \frac{dt_1}{dt_2}$***:***
  Compute $\lambda = \frac{j}{N}$
  Compute $\mathbf{D}_p^\nu$ according to the time scheme family
  Impose velocity continuity between the domains: $\mathbf{v}_{p+1}^\nu = \lambda \mathbf{v}_i^\varphi + (1-\lambda)\,\mathbf{v}_{i+1}^\varphi$
  Compute displacement in subdomain $\mathbf{u}_{p+1}^\nu = {C^\nu}^{-1}\left(\mathbf{v}_{p+1}^\nu - \mathbf{D}_p^\nu\right)$
  (and acceleration if needed according to time scheme family of subdomain ν).
  For each subdomain $\textcircled{m}$=ν to $\textcircled{M}$
    - ***Call*** subdomain $\textcircled{m}$ with kinematic at its boundary:
      $\mathbf{u}_{p+1}^{\textcircled{m}}$, $\mathbf{v}_{p+1}^{\textcircled{m}}$ (and $\mathbf{a}_{p+1}^{\textcircled{m}}$ or $\mathbf{u}_{p+\theta}^{\textcircled{m}}$ and $\mathbf{v}_{p+\theta}^{\textcircled{m}}$ and $\mathbf{v}_p^{\textcircled{m}}$ according to family
    - ***Update*** subdomain internal variables
    - ***Return*** resisting force (or impulsion) in $p+1$:
      $\mathbf{F}_{p+1}^{\textcircled{m}}$ and global tangent operator from subdomain $\textcircled{m}$: $\tilde{\mathbf{K}}$ and $\tilde{\mathbf{S}}$
    - ***Set*** the incremental terms of the algorithmic tangent operator: $\mathbf{\Sigma}_H$ and $\mathbf{\Sigma}_T$ to 0
    - ***Initialise*** algorithmic condensation operators:
      $H_p^{\textcircled{m}}$ according to equation 83 and $\mathbf{T}_p$ according to equation 90
    - ***For*** $p = 1$ ***to*** j
      $\mathbf{\Sigma}_H = \mathbf{\Sigma}_H + \left(\tilde{\mathbf{S}}{\mathbf{M}^\nu}^{k-1}\mathbf{Q}^\nu\right) H_{j-(p-1)}^\nu$
      $\mathbf{\Sigma}_T = \mathbf{\Sigma}_T + \left(\tilde{\mathbf{S}}{\mathbf{M}^\nu}^{k-1}\mathbf{Q}^\nu\right) \mathbf{T}_{j-(p-1)}$
    - ***End For***
    Compute $\mathbf{T}_{p+1}$ and H_{p+1}^ν and then $\tilde{\mathbf{k}}_{p+1}$ according to equation 90
    Compute $\mathbf{F}_{i+1}^\nu$ according to equation 80
  End For
End For
(vii) ***Update*** internal variables of all the subdomains
(viii) ***Update*** displacement, velocity and acceleration for next time step i of subdomain φ

Algo 5.1: Algorithm of the interface element for coupling time schemes in multi-time stepping; computation of the algorithmic tangent operator

- A second simulation is run by considering a Newmark time scheme with $\gamma = 1/2$, $\beta = 1/4$ in both subdomains and with a coarse time step $\Delta t = 1.10^{-1}$ in subdomain φ, and with a fine time step $dt = 1.10^{-2}$ in subdomain ν ($m = \frac{\Delta t}{\delta t} = 10$);

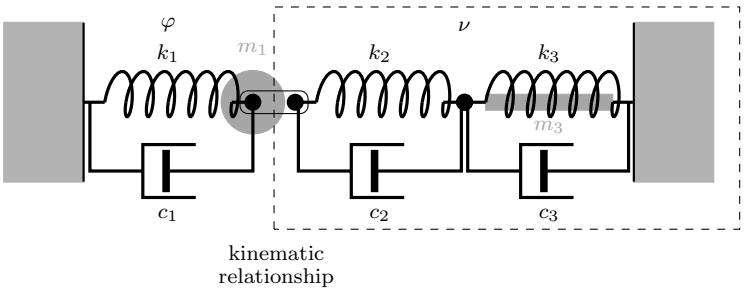

Figure 4: Numerical representation of the simple mass-dashpot-spring model

- A third simulation is carried out using a Newmark scheme in subdomain φ (time step $\Delta t = 1.10^{-1}$, $\gamma = 1/2$, $\beta = 1/4$) and a Euler+θ time scheme in subdomain ν (time-step $dt = 1.10^{-2}$, $\theta = 1/2$ and then $m = \frac{\Delta t}{\delta t} = 10$.

Appendix A lists the details of the numerical implementation for Newmark/Newmark and Newmark/Euler couplings, along with a definition of the various operators needed to build the algorithmic static condensation.

The response, in terms of displacement, velocity and acceleration, at all system nodes are presented in comparison with the reference simulation. Moreover, the algorithmic tangent operator demonstrated in this paper leads to global Newton-Raphson algorithm convergence in just 1 iteration.

The comparison between reference and proposed algorithm with substructuring of the resolution results in a perfect match for the displacements, velocities and accelerations for the interface nodes as well as for the internal node inside subdomain ν.

Figure 6 shows the order of accuracy for displacement, velocity and acceleration, calculated with $m = 10$ as:

$$\tau_\alpha = \sum_{DOF} \max_i \left(\frac{|\alpha^{th}_{DOF} - \alpha^{num}_{DOF}|}{\alpha^{th}_{DOF}} \right) \tag{93}$$

The order of accuracy of the coupling algorithm is equal to 2: $\tau_u = \tau_v = \tau_a = \mathcal{O}(dt^2)$.

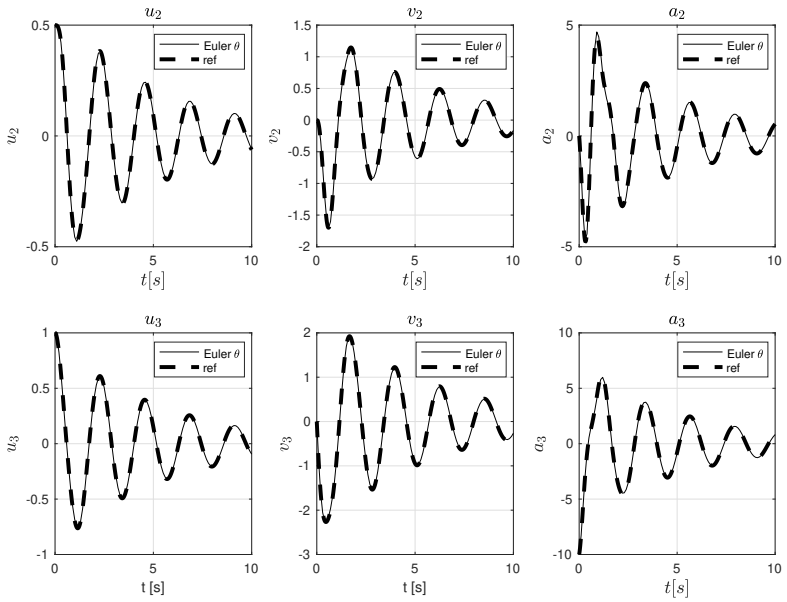

Figure 5: Numerical results, comparison of the displacements, velocities and accelerations between a reference simulation in full Newmark ($dt = 1.10^{-2}$) (ref) and a coupling with Newmark ($dt = 1.10^{-1}$) for subdomain φ and Euler+θ ($dt = \frac{1}{10}1.10^{-1}$) for subdomain ν.

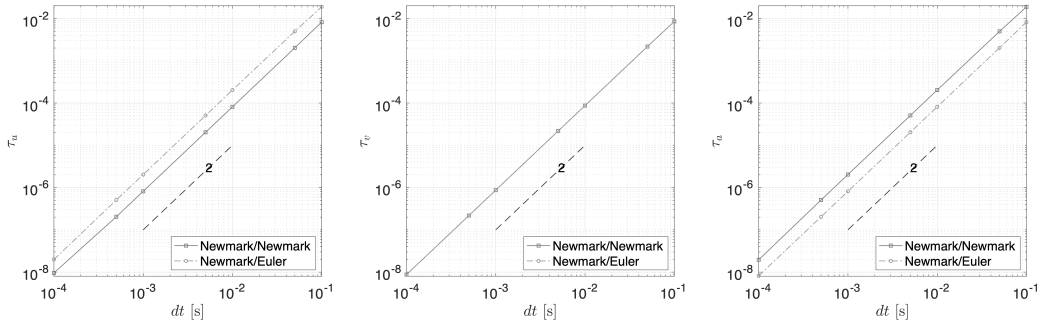

Figure 6: Order of accuracy for displacement, velocity and acceleration in the case of the 2 degrees-of-freedom system for a Newmark/Newmark coupling and a Newmark/Euler coupling with $m = 10$

7. Numerical simulations

7.1. Elastic rod under dynamic axial laoding

From the work of a few authors, e.g. Smolinski (1992a), Belytschko et al. (1979), Wu and Smolinski (2000) and Liu and Belytschko (1982), an elastic

rod has been studied with a different element size. This test problem is a one-dimensional elastic rod with 2 subdomains and different-sized mesh, time scheme and time step for the integration step. Like in Smolinski (1992a), the mesh has been chosen to represent an 11-m long rod using 10 elements of length $L = 1m$ (subdomain φ) and 10 elements of length $L = 0.1m$ (subdomain ν) (Fig. 7a). The subdivision is performed with the algorithm presented in this paper by duplicating the node at the interface (Fig. 7b).

The rod was fixed at its right-end extremity, and a force was applied instantaneously and held constant in order to create an axial stress in the left-end extremity of the rod of: $\sigma = 0.01Pa$.

The material parameters were chosen so that the wave speed was $c = 1m/s$ (Young's modulus $E = 1Pa$ and density $\rho = 1kg/m^3$). In the following discussion, in order to remain consistent with the results of Smolinski (1992a), the mass will be considered as lumped at the nodes (Note: the elementary mass matrix with off-diagonal terms could nevertheless be easily used).

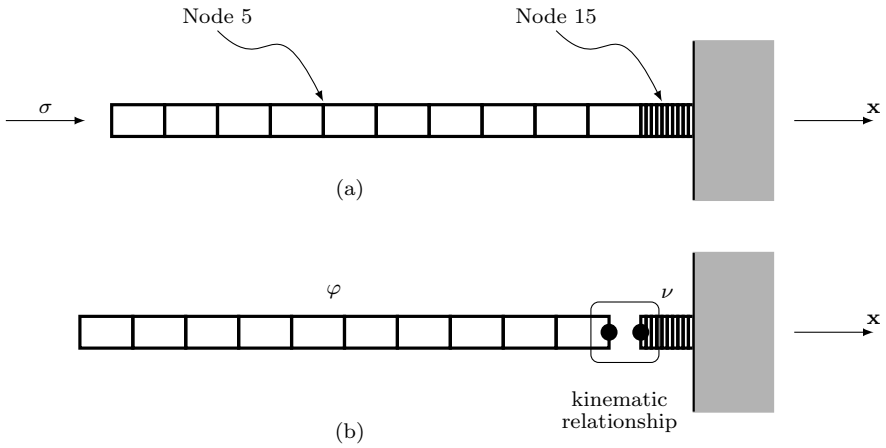

Figure 7: (a) Mesh and (b) domain subdivision of the elastic rod subjected to axial wave propagation

Two reference simulations were run with a Newmark time scheme and a time-step $dt = 0.075s$, on the one hand, and $dt = 0.0075s$ on the other in order to both obtain two reference solutions and underscore the effect of the time step.

The domain decomposition algorithm was then applied in maintaining the Newmark time scheme ($\beta_1 = 1/2$ and $\gamma_1 = 1/4$), for the part with the element of length $L = 1$ and with a time step $dt_1 = 0.075s$, along with a

Euler+θ time scheme ($\theta_2 = 1/2$) for the part with $L = 0.1m$ and a time step divided by $m = 10$ ($dt_2 = \frac{1}{10} dt_1 = 0.0075s$).

For all these simulations, the algorithmic tangent operator was used and led to convergence in just 1 iteration.

A comparison between the reference case and the subdomain coupling for the axial velocity of node 5 is given in Figure 8a and that for node 15 in figure 8b.

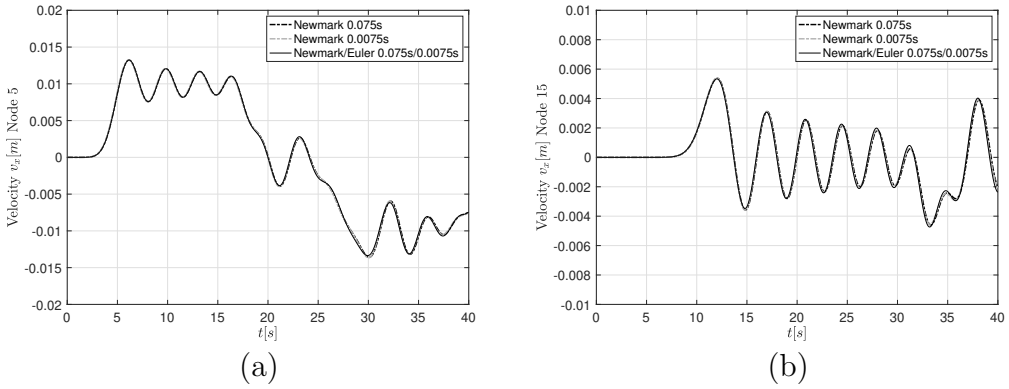

Figure 8: Comparison of the axial velocities between a full Newmark and Newmark/Euler+θ coupling for $m = 10$ for node 5 and 15

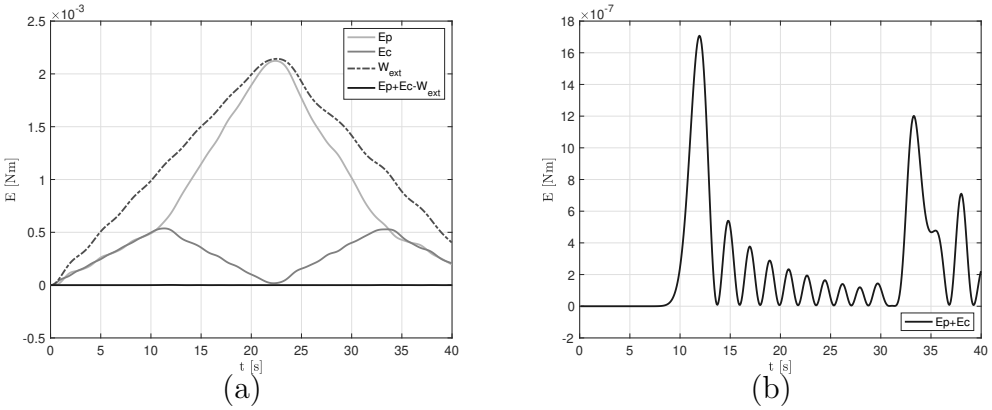

Figure 9: (a) Energy conservation and (b) $E_m(t) - E_m(0)$ of the system when considering the time scheme coupling for $m = 10$

Only a small difference is observed between the 2 reference cases and the coupling algorithm; this is merely due to the time discretisation of the wave propagation phenomenon.

Figure 9a shows the evolution of total energy in the system, indicating the absence of dissipation in the system at the interface between subdomains, while Figure 9b displays the total energy residual.

7.2. Newmark and Euler+θ coupling using a complementary method for hard contact problems in non-smooth mechanics

7.2.1. Presentation of the structure

A portal frame subjected to the contact of a ball is set up in this section using complementarity non smooth mechanics methods for the contact (Fig. 10).

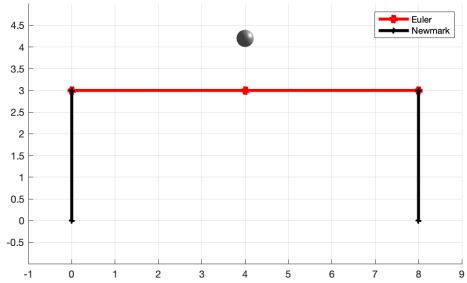

Figure 10: Portal frame with impacts using Euler+θ and complementary methods for the ball and horizontal beam linked with the 2 posts treated in Newmark.

The Newmark family is usually used in structural dynamic analysis for its numerical damping properties. The Euler+θ method is typically employed for complementary method Acary (2013) in order to solve hard contact problems. Some authors have tried to tackle this problem by using a complementary method within a Newmark family framework Wriggers (2006). Corrective terms are then needed in order to maintain exact energy during the impact time step.

For this reason, it can be most useful to couple these time schemes, thus providing a tool that allows combining hard contact applications within a Newmark framework for the rest of the structure.

The 2 posts and their masses have been modelled using a Newmark time scheme, whereas the transversal beam and ball have been modelled using a Euler+θ method with its complementarity algorithm.

For information, Appendix B shows the details of the implementation of complementarity problems to implicitly treat hard contacts within a Euler $+\theta$ framework.

7.2.2. Numerical testing and results

A comparison of the response of the portal frame and the ball trajectory was drawn in terms of both velocities and displacements, in considering a reference configuration treated with full Euler$+\theta$: the configuration using 2 posts was treated with Newmark and the horizontal beam and ball in Euler$+\theta$, as presented in Figure 10. In both configurations the time step is the same and equal to $dt = 5.10^{-3}s$ in order to compare the scheme coupling between a second-order time scheme (Newmark) and a first-order one (Euler).

The restitution coefficient $e = 1$, hence no damping at the point of impact was taken into account. The Young's modulus of the beams is $E = 30GPa$, with cross-sections $b = 0.5m$ and $h = 0.1m$, and density $\rho = 2500kg/m^3$. The posts were discretised using 1 Bernoulli linear beam element and the horizontal beam as 2 Bernoulli linear beam elements at the contact node, with the ball in the middle. An additional mass was considered at the middle of the horizontal beam $M_0 = 300kg$. The ball mass $M_{ball} = 200kg$.

Figure 11a offers a comparison of the displacements and 11b compares the velocities of the ball and middle of the horizontal beam for the two configurations (reference and coupling), which do match perfectly.

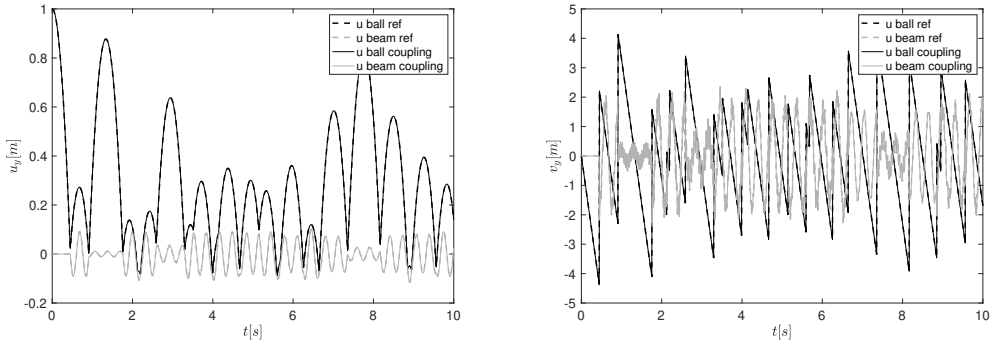

(a) (b)

Figure 11: Comparison of the displacements (a) and velocities (b) between a full Euler$+\theta$ method and coupling of the time schemes for $m = 1$

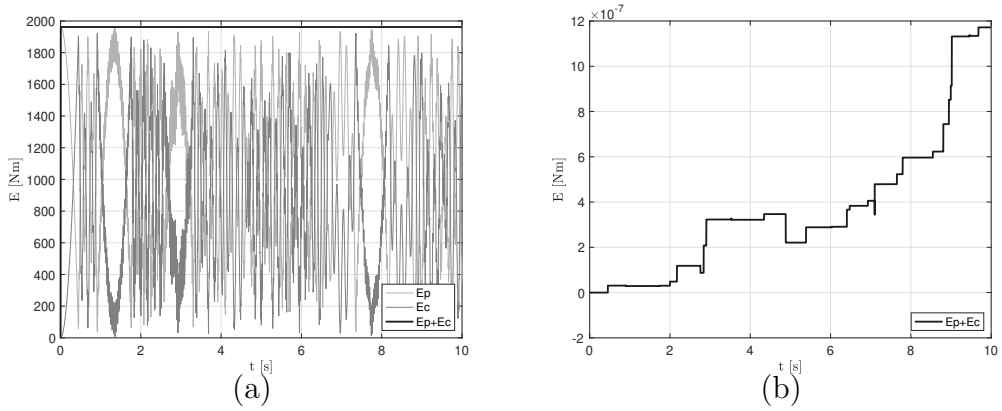

Figure 12: (a) Energy conservation and (b) $E_m(t) - E_m(0)$ of the coupling algorithm for $m = 1$

Lastly, Figure 12a shows the evolution in both kinematic and potential energy. The initial conditions lead to a potential energy at the beginning of the system equal to $E_p = M_{ball}gH = 1962Nm$, which remains perfectly constant and moreover demonstrates that the algorithm is able to maintain mechanical energy without any dissipation. Figure 12b displays the total energy residual.

7.3. Nonlinear behaviour of a pendulum attached on a frame

The nonlinear behaviour of a pendulum with large displacements will be discussed in this section. Its mass equilibrium has been treated inside an element with an internal degree of freedom (rotation of the pendulum) that can be seen as subdomain ν and attached to an elastic portal frame (subdomain φ). Three masses were attached to the portal frame in order to generate dynamic forces inside the structure.

This example is nonlinear and requires 2 or 3 iterations in order to obtain convergence with the tangent operator when the pendulum is being managed at the global scale. The pendulum has a mass $m_p = 3$ and its length is set equal to $L_p = 1$. An initial condition on the angle of the pendulum of $\beta = -\frac{\pi}{4}$ has been considered. This initial condition led to a potential energy at the beginning of the system equal to $E_p = m_p g L_p \left(1 - \cos\left(-\frac{\pi}{4}\right)\right) = 8.61$.

Subdomain φ is calculated using a Newmark time scheme.

In this set-up, two distinct applications are provided:

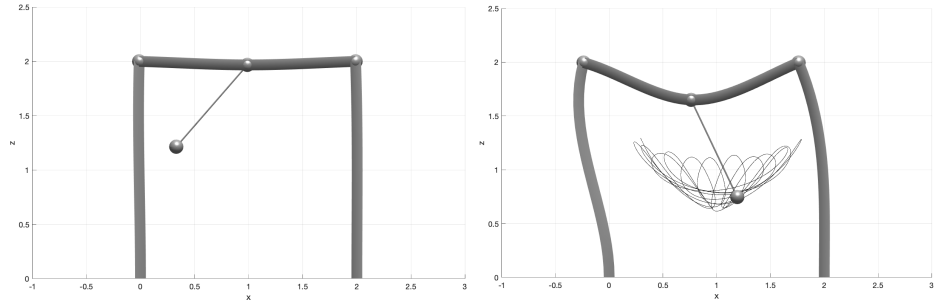

Figure 13: Nonlinear pendulum system attached to a frame: Representation of the deformed shape at a given time step, and the trajectory of its mass when the pendulum is subjected to an initial angle of $-\frac{\pi}{4}$

- the dynamic internal equilibrium of subdomain ν is calculated with a Newmark time scheme, and
- use of a Euler $+\theta$ time scheme

Both applications are treated using a finer time step in the pendulum domain with $m = 15$.

Figure 14 exhibits the evolution of the angular values, and velocity and trajectory of the pendulum mass compared to a reference. This reference case has been simulated considering just 1 domain using Newmark and the equilibrium of the pendulum assembled in the global system (i.e. no substructuring).

The coupling between both domains yields convergence in 2 or 3 iterations, as is the case for the reference system, thus showing that the algorithmic tangent operator proposed in this paper (in Equation 70) is a very good approximation, even in the case of asynchronous simulations.

Figure 16a shows the evolution in total energy, which reveals that the algorithm does not dissipate energy at the interface; Figure 16b provides the total energy residual.

7.4. 2D plane stress beam with J2 plasticity constitutive law

This section considers a 2D cantilever beam with a nonlinear constitutive law (plane stress J2 plasticity, see Simo and Hughes (1998)) . As previously presented in Combescure and Gravouil (2001), steel material is considered with a Young's modulus $E = 210GPa$, a Poisson's ratio $\nu = 0.2$, a yield stress

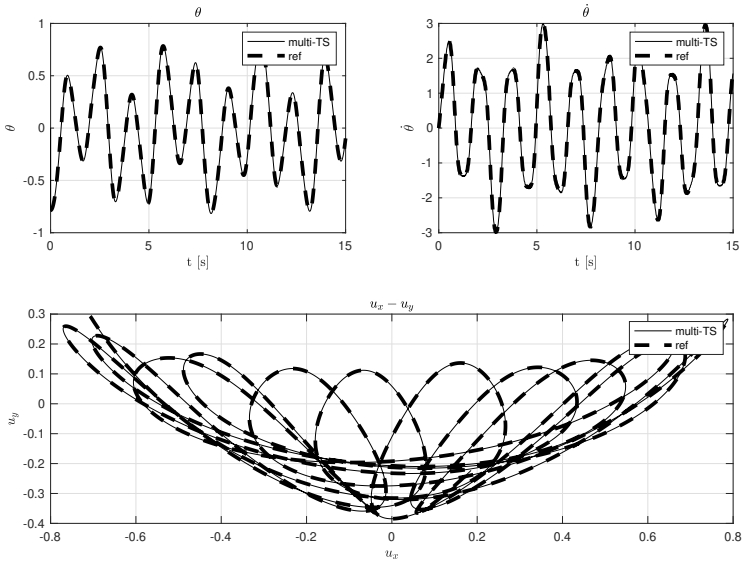

Figure 14: Comparison of the pendulum mass trajectories between full Newmark and Newmark/Newmark coupling with multi-time stepping $m = 15$

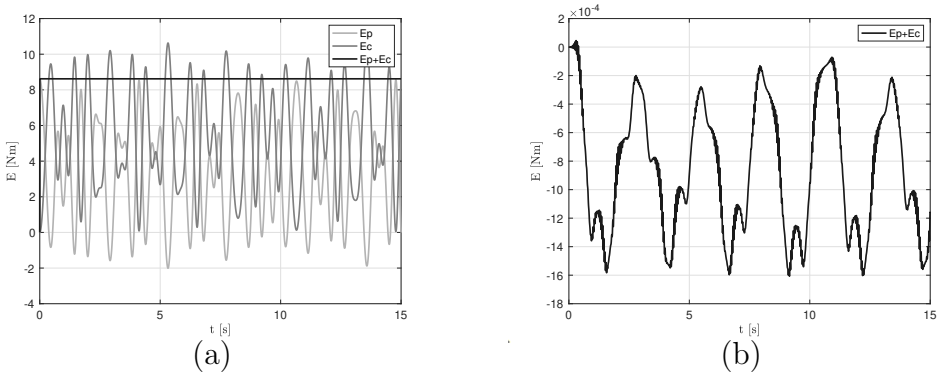

Figure 15: (a) Energy evolution and (b) $E_m(t) - E_m(0)$ in the pendulum/frame system for the Newmark/Newmark time scheme coupling with multi-time stepping $m = 15$

$f_y = 500MPa$, an isotropic hardening parameter $H = 20GPa$, and a density $\rho = 7800kg/m^3$. A constant vertical force $F_y = -5MN$ is instantaneously applied to the left end of the beam and then released at $t = 0.1s$ (to show that nonlinear permanent strains are generated). The displacement at this

point is then calculated using a reference simulation (without coupling) in Newmark ($dt = 2.10^{-4}s$), and the proposed coupling algorithm with a left-half part of the beam is treated with Newmark ($dt = 2.10^{-4}s$) while the right-half part relies on Euler+θ ($dt = \frac{2.10^{-4}}{5}s$).

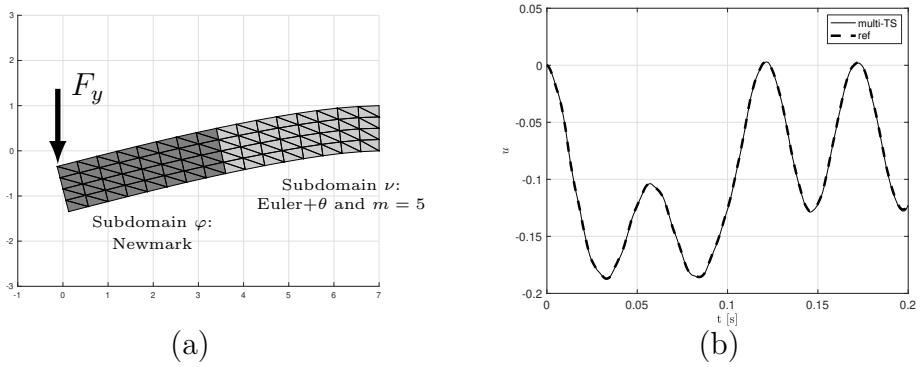

Figure 16: (a) 2D representation of a cantilever beam with plane stress J2 plasticity; (b) Vertical displacement at the left end of the beam for a Newmark/Euler θ time scheme coupling with multi-time stepping $m = 5$ and for a full Newmark reference system

The comparison between both simulations shows a perfect match of the displacement. Moreover, the strong convergence properties are maintained thanks to the correct evaluation of the algorithmic tangent operator, even though material nonlinearities are developed.

8. Conclusion and perspectives

This paper has presented a new primal HATI coupling procedure based on domain decomposition and a sub-structuring method. The interface between subdomains at these nodes is taken into account by: "duplicating" node kinematics at the subdomain interface, writing kinematic continuity in velocity, and allowing for the solution of subdomains independently inside a global equilibrium of a master subdomain. The time schemes used in the various subdomains can be explicit or even both implicit. An exact tangent algorithmic operator is provided for implicit/implicit couplings as well as for multi-time stepping problems, in which case the algorithmic tangent operator (to maintain quadratic convergence) originates from a generalisation of the static condensation of operators condensed at the interface nodes, a process referred to as algorithmic static condensation.

An analysis based on a simple 2 degrees-of-freedom system shows that the coupling has an error in displacement, velocity and acceleration in $\mathcal{O}(dt^2)$.

The comparison of a reference configuration and multi-scheme coupling has been performed through 3 distinct applications coupling Newmark/Newmark and Newmark/Euler+θ time schemes under asynchronous conditions for both linear and nonlinear problems. The coupling between Newmark and Euler+θ is furthermore highly beneficial, even in a synchronous manner, for a very simple treatment of dynamic impact within the framework of non-smooth mechanics. Indeed, the attractive properties of the Euler time scheme for linear complementarity algorithms can be harnessed while maintaining the good stability and damping properties of Newmark families for the rest of the structures.

In all three applications, the comparison between couplings and the reference shows very good agreement and ensures a quadratic convergence thanks to the evaluation of the exact algorithmic tangent operator.

This method, which is not intrusive as an interface element between the subdomains, can be easily written and ultimately implemented as a user element in a commercial finite element code. The method is very suitable for multiscale modelling problems where subdomains (macro-element) present a time dependency and require internal time discretisation to ensure internal dynamic equilibrium.

Further work is still required to evaluate the method's accuracy and stability on more complex problems and to improve accuracy when using non-smooth hard contact mechanics in an asynchronous manner. In addition, other couplings considering other time schemes could be similarly performed and are currently under development as the coupling using implicit/explicit time schemes (central difference method or Euler+$\theta = 0$ and θ within $\left[0, \frac{1}{2}\right]$). In order to complete the dynamic analysis, an application of this method using an HHT scheme is also possible and would need to be validated. Finally, the coupling of different subdomains in dynamics raises the question of taking Rayleigh damping into account independently in each part. This point deserves further investigations, especially when tangent stiffness is used to update this damping.

Appendix A. The Spring Dashpot Mass model

Appendix A.1. Newmark/Newmark coupling

The system of subdomain ν is composed of 1 internal degree of freedom and 2 boundary conditions (I is the left-end node and J the right-end node). I is then connected to subdomain φ and constitutes the interface between the subdomains. Node J is actually a boundary condition of the system, and its kinematic variable is constant and equal to 0 at all time steps.

Mass m_3 is a spread over the spring, thus generating a mass matrix $\mathbf{m_3} = \begin{bmatrix} m_3 & -m_3 \\ -m_3 & m_3 \end{bmatrix}$ (as it is the case for a bar element). But in this case, since the boundary condition is fixed at the right-end node (node J: $u_J = 0$), it would be exactly the same to consider a concentrated mass m_3 at the internal node of subdomain ν.

The internal equilibrium equation of subdomain ν at the time step $p+1$ can be written as follows:

$$\begin{bmatrix} 0 & 0 & 0 \\ 0 & m_3 & -m_3 \\ 0 & -m_3 & m_3 \end{bmatrix} \begin{bmatrix} a_{p+1}^{I\nu} \\ a_{p+1}^{\nu^{(k)}} \\ a_{p+1}^{J\nu} \end{bmatrix} + \begin{bmatrix} c_2 & -c_2 & 0 \\ -c_2 & c_2 & 0 \\ 0 & 0 & 0 \end{bmatrix} \begin{bmatrix} v_{p+1}^{I\nu} \\ v_{p+1}^{\nu^{(k)}} \\ v_{p+1}^{J\nu} \end{bmatrix} + \begin{bmatrix} k_2 & -k_2 & 0 \\ -k_2 & k_2 & 0 \\ 0 & 0 & 0 \end{bmatrix} \begin{bmatrix} u_{p+1}^{I\nu} \\ u_{p+1}^{\nu^{(k)}} \\ u_{p+1}^{J\nu} \end{bmatrix} = \begin{bmatrix} f_{p+1}^{I\nu} \\ 0 \\ f_{p+1}^{J\nu} \end{bmatrix} \tag{A.1}$$

Such a system is solved in this first example using a Newmark time scheme written with displacement as the main unknown. The internal equilibrium is resolved using a Newton Raphson method that ultimately provides: the kinematic of the internal degree of freedom, the resisting force at node I, and the global tangent matrix of subdomain ν.

The global tangent operator here is constant and composed by assembling the various elements of subdomain ν as:

$$\tilde{\mathbf{K}} = \begin{bmatrix} k_2 + c_2 C^\nu & -(k_2 + c_2 C^\nu) & 0 \\ -(k_2 + c_2 C^\nu) & k_2 + c_2 C^\nu + m_3 A^\nu & -m_3 A^\nu \\ 0 & -m_3 A^\nu & m_3 A^\nu \end{bmatrix} \tag{A.2}$$

This operator is ordered in the following manner:

$$\mathbf{U}_{p+1}^\nu = \begin{bmatrix} u_{p+1}^{I\nu} \\ u_{p+1}^{\nu^{(k)}} \\ u_{p+1}^{J\nu} \end{bmatrix} \tag{A.3}$$

The internal equilibrium equation of subdomain ν (2nd row of the system) to be solved using the Newton Raphson method is therefore given by

Equation A.4. In this equation, the boundary condition at node J is taken into account and then $u_{p+1}^{J\nu}$ is equal to 0. In considering this condition, then only $u_{p+1}^{I\nu}$ remains, as imposed by subdomain φ (see Equation 53), which is why the I index has been omitted for the sake of simplification):

$$R^{(k)} = k_2 u_{p+1}^{\nu} + c_2 v_{p+1}^{\nu} - k_2 u_{p+1}^{\nu^{(k)}} - c_2 v_{p+1}^{\nu^{(k)}} - m_3 a_{p+1}^{\nu^{(k)}} = 0 \tag{A.4}$$

which can be written as:

$$R^{(k)} = (k_2 + c_2 C^{\nu})\, u_{p+1}^{\nu} - (k_2 + c_2 C^{\nu} + m_3 A^{\nu})\, u_{p+1}^{\nu^{(k)}} + c_2 D_{p+1}^{\nu} - c_2 D_p^{\nu^{(k)}} - m_3 B_p^{\nu^{(k)}} = 0 \tag{A.5}$$

For this simple problem, the Newton Raphson method will obviously converge in just a single iteration, making it possible to find $u_{p+1}^{\nu^{(k)}}$ with the previous residual equation and deduce the resisting force at the interface with the first equation of the system.

If the internal computation within subdomain ν is subdivided into $p+1$ time steps within a single time step of domain φ, then the calculation of the tangent matrix involves the differential of the equilibrium equation and thus the derivatives of $D_p^{\nu^{(k)}}$ and $B_p^{\nu^{(k)}}$ which are no longer null (whereas they would be null if the time steps of subdomain ν and subdomain φ had been the same). This dependency brings up the $\tilde{\mathbf{S}}$ matrix, as shown in the previous sections and which would be valid in this example:

$$\tilde{\mathbf{S}} = \begin{bmatrix} c_2 & 0 & -c_2 & 0 & 0 & 0 \\ -c_2 & 0 & c_2 & m_3 & 0 & -m_3 \\ 0 & 0 & 0 & -m_3 & 0 & m_3 \end{bmatrix} \tag{A.6}$$

This matrix is ordered as follows:

$$\mathbf{W}_p^{\nu} = {}^t \begin{bmatrix} D_p^{I\nu} & B_p^{I\nu} & D_p^{\nu^{(k)}} & B_p^{\nu^{(k)}} & D_p^{J\nu} & B_p^{J\nu} \end{bmatrix} \tag{A.7}$$

Knowing $\tilde{\mathbf{K}}$ and $\tilde{\mathbf{S}}$, it is straightforward to program the operators H_{p+1}^{ν}, then $\mathbf{T}_{p+1}$, and subsequently the algorithmic tangent matrix $\tilde{\mathbf{k}}_{p+1}$ at each time step $p+1$.

In practice, these calculations stem from the resolution of the internal equation A.5, which thus makes it possible to determine at each step p the displacement value of the internal degrees of freedom $u_{p+1}^{\nu^{(k)}}$ according to the displacement imposed at the interface u_{p+1}^{ν}.

By reintroducing this value at each step in the other two equations, the algorithmic tangent operator is obtained as demonstrated in the previous section.

Appendix A.2. Newmark/Euler+θ coupling

The internal equilibrium equation of subdomain ν at the time step $p+1$ using the Euler+θ method can be written as follows:

$$\begin{bmatrix} 0 & 0 & 0 \\ 0 & m_3 & -m_3 \\ 0 & -m_3 & m_3 \end{bmatrix} \begin{bmatrix} v_{p+1}^{I\nu} - v_p^{I\nu} \\ v_{p+1}^{\nu^{(k)}} - v_p^{\nu^{(k)}} \\ v_{p+1}^{J\nu} - v_p^{J\nu} \end{bmatrix} + dt \begin{bmatrix} c_2 & -c_2 & 0 \\ -c_2 & c_2 & 0 \\ 0 & 0 & 0 \end{bmatrix} \begin{bmatrix} v_{p+\theta}^{I\nu} \\ v_{p+\theta}^{\nu^{(k)}} \\ v_{p+\theta}^{J\nu} \end{bmatrix} + dt \begin{bmatrix} k_2 & -k_2 & 0 \\ -k_2 & k_2 & 0 \\ 0 & 0 & 0 \end{bmatrix} \begin{bmatrix} u_{p+\theta}^{I\nu} \\ u_{p+\theta}^{\nu^{(k)}} \\ u_{p+\theta}^{J\nu} \end{bmatrix} = \begin{bmatrix} p_{p+1}^{I\nu} \\ 0 \\ p_{p+1}^{J\nu} \end{bmatrix} \tag{A.8}$$

where $p_{p+1}^{I\nu}$ returned to subdomain φ as a reaction of the boundary conditions are pulses (and not forces)

According to equation 82, matrix $\tilde{\mathbf{S}}$ can be expressed as:

$$\tilde{\mathbf{S}} = \begin{bmatrix} dt_2(1-\theta\nu)c_2 - [dt_2(1-\theta\nu)]^2 k_2 & -dt_2(1-\theta\nu)c_2 + [dt_2(1-\theta\nu)]^2 k_2 & 0 & -dt_2 C^{\nu^{-1}} k_2 & dt_2 C^{\nu^{-1}} k_2 & 0 \\ -dt_2(1-\theta\nu)c_2 + [dt_2(1-\theta\nu)]^2 k_2 & -m_3 + dt_2(1-\theta\nu)c_2 - [dt_2(1-\theta\nu)]^2 k_2 & m_3 & dt_2 C^{\nu^{-1}} k_2 & -dt_2 C^{\nu^{-1}} k_2 & 0 \\ 0 & m_3 & -m_3 & 0 & 0 & 0 \end{bmatrix} \tag{A.9}$$

which is ordered as:

$$\mathbf{W}_p^{\nu} = {}^t \begin{bmatrix} v_p^{I\nu} & v_p^{\nu^{(k)}} & v_p^{J\nu} & D_p^{I\nu} & D_p^{\nu^{(k)}} & D_p^{J\nu} \end{bmatrix} \tag{A.10}$$

and can then be reordered as:

$$\mathbf{W}_p^{\nu} = {}^t \begin{bmatrix} v_p^{I\nu} & D_p^{I\nu} & v_p^{\nu^{(k)}} & D_p^{\nu^{(k)}} & v_p^{J\nu} & D_p^{J\nu} \end{bmatrix} \tag{A.11}$$

yielding:

$$\tilde{\mathbf{S}} = \begin{bmatrix} dt_2(1-\theta\nu)c_2 - [dt_2(1-\theta\nu)]^2 k_2 & -dt_2 C^{\nu^{-1}} k_2 & -dt_2(1-\theta\nu)c_2 + [dt_2(1-\theta\nu)]^2 k_2 & dt_2 C^{\nu^{-1}} k_2 & 0 & 0 \\ -dt_2(1-\theta\nu)c_2 + [dt_2(1-\theta\nu)]^2 k_2 & dt_2 C^{\nu^{-1}} k_2 & -m_3 + dt_2(1-\theta\nu)c_2 - [dt_2(1-\theta\nu)]^2 k_2 & -dt_2 C^{\nu^{-1}} k_2 & m_3 & 0 \\ 0 & 0 & m_3 & 0 & -m_3 & 0 \end{bmatrix} \tag{A.12}$$

The operators needed to collect the time scheme parameters can thus be written as:

$$\mathbf{M}^{\nu} = \begin{bmatrix} 0 & 0 & 0 & 0 & 0 & 0 \\ 0 & 1 & 0 & 0 & 0 & 0 \\ 0 & 0 & 0 & 0 & 0 & 0 \\ 0 & 0 & 0 & 1 & 0 & 0 \\ 0 & 0 & 0 & 0 & 0 & 0 \\ 0 & 0 & 0 & 0 & 0 & 1 \end{bmatrix} \tag{A.13}$$

$$\mathbf{Q}^{\nu} = \begin{bmatrix} 1 & 0 & 0 \\ -\left[1 + C^{\nu} dt_2 \left(1 - \theta^{\nu}\right)\right] & 0 & 0 \\ 0 & 1 & 0 \\ 0 & -\left[1 + C^{\nu} dt_2 \left(1 - \theta^{\nu}\right)\right] & 0 \\ 0 & 0 & 1 \\ 0 & 0 & -\left[1 + C^{\nu} dt_2 \left(1 - \theta^{\nu}\right)\right] \end{bmatrix} \tag{A.14}$$

These operators are subsequently used to calculate the algorithmic tangent operators at every time-step $p+1$, as demonstrated in Equations 90 and 92.

Appendix B. Complementarity problems

Appendix B.0.1. Internal complementary problem with one contact in subdomain ν

The linear Complementary Problem (LCP) Acary (2013) constitutes a very interesting and robust method for handling hard contacts and non-smooth mechanics. In the hard contact problem, the relative velocity between nodes is discontinuous. Use of a second-order time scheme family ultimately leads to numerical difficulties. A first-order time scheme is better for this kind of problem; it is associated with the complementary method and allows imposing velocity discontinuity by adding a complementary term into the dynamic equilibrium (which becomes the new unknown during contact).

The problem to be solved (for a linear structure) is then:

$$\mathbf{M}(\mathbf{v}_{i+1} - \mathbf{v}_i) + dt\mathbf{K}\mathbf{u}_{i+\theta} = {}^{t}\mathbf{H} \underbrace{dt \times r_{i+1}}_{p_{i+1}} + dt\mathbf{F}^{ext}_{i+\theta} \tag{B.1}$$

where:

- **H** is a rectangular-shaped matrix containing the kinematic links between the degrees of freedom and the possibility of 2 nodes being in contact;

- p_{i+1} is the percussion (complementary term) to be added to the dynamic equation in order to fulfil equilibrium at the contact nodes (resisting force r_{i+1}) and moreover required mathematically as an unknown in order to impose velocity discontinuity.

Note:. In this section, the kinematic conditions are linear and **H** is thus held constant.

The relative velocity, gap function and Signorini conditions that define the contact are written as follows:

$$\left\{ \begin{array}{l} U_{i+1} = \mathbf{H}\mathbf{v}_{i+1} \\ g_{N_{i+1}} = \mathbf{H}\mathbf{u}_{i+1} + b \ (linearhere) \\ if \quad \hat{g}_{N_{i+1}} \leq 0, \ 0 \leq U_{i+1} + eU_i \perp p_{i+1} \geq 0 \end{array} \right. \tag{B.2}$$

where e is the Newton's restitution coefficient, and $\hat{g}_{N_{i+1}}$ the explicit prediction of contact, which can be expressed as follows: $\hat{g}_{N_{i+1}} = g_i + dt\gamma U_i$ (with $\gamma = \frac{3}{2}$)

With all these ingredients, the equilibrium equation can be rewritten as:

$$\mathbf{M}(\mathbf{v}_{i+1} - \mathbf{v}_i) + dt\mathbf{K}((1-\theta)\mathbf{u}_i + \theta\mathbf{u}_{i+1}) = \ {}^t\mathbf{H}p_{i+1} + dt\mathbf{F}^{ext}_{i+\theta} \tag{B.3}$$

which ultimately yields:

$$\left\{ \begin{array}{l} \underbrace{\left(\mathbf{M} + dt^2\theta^2\mathbf{K}\right)}_{\hat{\mathbf{M}}}\mathbf{v}_{i+1} = \ {}^t\mathbf{H}p_{i+1} + \underbrace{dt\mathbf{F}^{ext}_{i+\theta} + \left(\mathbf{M} - dt^2\mathbf{K}\theta(1-\theta)\right)\mathbf{v}_i - h\mathbf{K}\mathbf{u}_i}_{\hat{\mathbf{F}}} \\ U_{i+1} = \mathbf{H}\mathbf{v}_{i+1} \\ then \quad LCP : if \quad \hat{g}_{N_{i+1}} \leq 0, \ 0 \leq U_{i+1} + eU_n \perp p_{i+1} \geq 0 \quad to \quad be \quad solved \end{array} \right. \tag{B.4}$$

Then:

$$\underbrace{\mathbf{H}\hat{\mathbf{M}}^{-1} \ {}^t\mathbf{H}}_{W}p_{i+1} + \underbrace{\mathbf{H}\hat{\mathbf{M}}^{-1}\hat{\mathbf{F}}}_{q} - U_{i+1} = 0 \tag{B.5}$$

In other words, the following equation must be solved Acary (2013):

$$\left\{ \begin{array}{l} Wp_{i+1} + q - U_{i+1} = 0 \\ \ 0 \leq U_{i+1} + eU_i \perp p_{i+1} \geq 0 \end{array} \right. \tag{B.6}$$

To solve this system, it is necessary to calculate the percussion using Equations B.6. Signorini's condition will instruct us to take the maximum between 0 and the calculated percussion value (because it must be positive). Once this percussion has been calculated, provided it exists and is nonzero, it is reinjected into Equation 1 of the system in B.4 in order to calculate the actual velocity generated by this percussion over the time step.

$$\begin{cases} p_{i+1} = max\left(0, -W^{-1}(q + eU_i)\right) \\ \mathbf{v}_{i+1} = \hat{\mathbf{M}}^{-1}\left[\ {}^{t}\mathbf{H}p_{i+1} + \hat{\mathbf{F}}\right] \end{cases} \tag{B.7}$$

In practice, the transfer of information between Newmark's and Euler's time schemes must therefore be performed using the displacements and velocities at time steps $i + \theta$ but also the velocity at time steps i and time steps $i + 1$. The reactions at the domain boundary are the pulses at $i + \theta$ (and not the forces at $i + 1$); moreover, they must be translated. It is the interface element for coupling the time schemes that must serve to calculate these quantities.

Appendix C. Pendulum equilibrium

The purpose of this chapter is to use the VPP* in order to write the equilibrium of a pendulum, as well as the resistance forces generated on the node where the pendulum is attached and which would be subjected to acceleration. The calculation of the tangent operator can then be derived and returned to the node by means of static condensation.

The displacements quantities are then:

$$\begin{cases} \vec{G_0G} = u\mathbf{X} + v\mathbf{Y} \\ \vec{A_0A} = u_A\mathbf{X} + v_A\mathbf{Y} \end{cases} \tag{C.1}$$

Appendix C.1. Displacements and velocities

Let u and v be the respective horizontal and vertical displacements of the pendulum mass within the Galilean reference frame. Let u_A and v_A be the displacements of the node A in the Galilean coordinate system and θ the angle that the rod makes with respect to the vertical.

A kinematic relationship exists between these 5 quantities, only 3 of which are independent. We are able to choose the independent set of kinematic parameters (u_A, v_A, θ) .

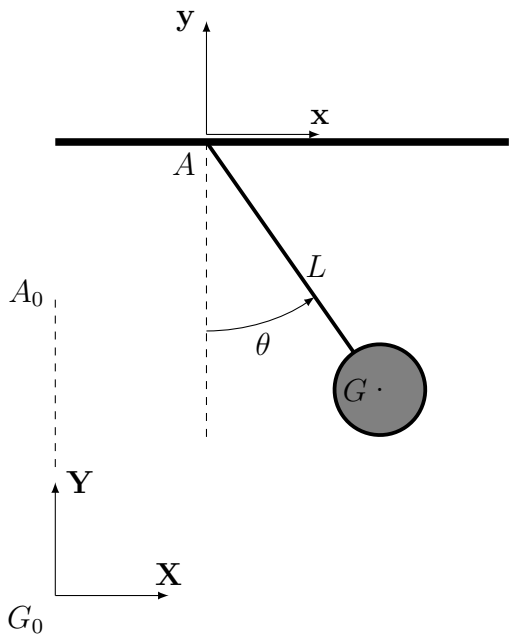

Figure C.17: Pendulum system attached at the top in system **x**, **y** in translation within a Galilean reference system **X** et **Y**

Hence:

$$\begin{cases} u = u_A + L\sin(\theta) \\ v = v_A + L\left(1 - \cos(\theta)\right) \end{cases} \tag{C.2}$$

In reality and in the following discussion, θ will denote an internal parameter whose value will be resolved by the internal equilibrium of the mass, which oscillates when node A is subjected to time dependant kinematics u_A and v_A (i.e. the kinematic parameters external to the element).

From the previous relations, we can therefore express the accelerations and associated virtual fields (tangents):

Thus:

$$\begin{cases} \ddot{u} = \ddot{u}_A + L\left[\ddot{\theta}\cos(\theta) - \dot{\theta}^2\sin(\theta)\right] \\ \ddot{v} = \ddot{v}_A + L\left[\ddot{\theta}\sin(\theta) + \dot{\theta}^2\cos(\theta)\right] \end{cases} \tag{C.3}$$

and its variations (used for VPP*):

$$\begin{cases} u^\star = \delta u = \delta u_A + L\delta\theta\cos(\theta) \\ v^\star = \delta v = \delta v_A + L\delta\theta\sin(\theta) \end{cases} \tag{C.4}$$

Appendix C.2. Equilibrium equation

Let X_A and Y_A be the node forces of the outside stem.

Applying VPP* to the system gives:

$$\begin{array}{rll} & \forall \mathbf{U}^\star, & \mathcal{P}^\star_{int} = \mathcal{P}^\star_{ext} \\ \Leftrightarrow & \forall \mathbf{U}^\star, & m\ddot{\vec{u}}.\vec{u}^\star = X_A u^\star_A + Y_A v^\star_A - P v^\star \\ \Leftrightarrow & \forall \mathbf{U}^\star, & m\ddot{u}u^\star + m\ddot{v}v^\star = X_A u^\star_A + Y_A v^\star_A - P v^\star \end{array} \tag{C.5}$$

$$\begin{aligned} \Leftrightarrow \forall \left(u^\star_A, v^\star_A, \theta^\star\right), \quad & m\left[\ddot{u}_A + L\left[\ddot{\theta}\cos(\theta) - \dot{\theta}^2\sin(\theta)\right]\right]\left[\delta u_A + L\delta\theta\cos(\theta)\right] \\ & + m\left[\ddot{v}_A + L\left[\ddot{\theta}\sin(\theta) + \dot{\theta}^2\cos(\theta)\right]\right]\left[\delta v_A + L\delta\theta\sin(\theta)\right] \\ & = X_A\delta u_A + Y_A\delta v_A - P\left[\delta v_A + L\delta\theta\sin(\theta)\right] \end{aligned} \tag{C.6}$$

Then:

$$\begin{bmatrix} u^\star_A & v^\star_A & \theta^\star \end{bmatrix} \begin{bmatrix} m\left[\ddot{u}_A + L\ddot{\theta}\cos(\theta) - L\dot{\theta}^2\sin(\theta)\right] \\ m\left[\ddot{v}_A + L\ddot{\theta}\sin(\theta) + L\dot{\theta}^2\cos(\theta)\right] + P \\ mL\cos(\theta)\ddot{u}_A + mL\sin(\theta)\ddot{v}_A + mL^2\ddot{\theta} + PL\sin(\theta) \end{bmatrix} = \begin{bmatrix} u^\star_A & v^\star_A & \theta^\star \end{bmatrix} \begin{bmatrix} X_A \\ Y_A \\ 0 \end{bmatrix} \tag{C.7}$$

The 3rd equation of the system (obtained thanks to $\theta^\star$) is indeed the internal equilibrium equation that allows calculating the internal equilibrium and deducing the angle $\theta(t)$ using a Newton-Raphson method.

$$mL\cos(\theta)\ddot{u}_A + mL\sin(\theta)\ddot{v}_A + mL^2\ddot{\theta} + PL\sin(\theta) = 0 \tag{C.8}$$

$$\begin{cases} m\left[\ddot{u}_A + L\ddot{\theta}\cos(\theta) - L\dot{\theta}^2\sin(\theta)\right] = X_A \\ m\left[\ddot{v}_A + L\ddot{\theta}\sin(\theta) + L\dot{\theta}^2\cos(\theta)\right] + P = Y_A \end{cases} \tag{C.9}$$

Appendix C.3. Resisting force

At each time step $i+1$ we are able to express these equilibrium equations, which can then be discretised using, for example, a Newmark method.

$$\underbrace{\begin{bmatrix} m\left[\ddot{u}_{A_{i+1}} + L\ddot{\theta}_{i+1}\cos(\theta_{i+1}) - L\dot{\theta}^2_{i+1}\sin(\theta_{i+1})\right] \\ m\left[\ddot{v}_{A_{i+1}} + L\ddot{\theta}_{i+1}\sin(\theta_{i+1}) + L\dot{\theta}^2_{i+1}\cos(\theta_{i+1})\right] + P \\ mL\cos(\theta_{i+1})\ddot{u}_{A_{i+1}} + mL\sin(\theta_{i+1})\ddot{v}_{A_{i+1}} + mL^2\ddot{\theta}_{i+1} + PL\sin(\theta_{i+1}) \end{bmatrix}}_{\mathbf{P}(\mathbf{U}_{i+1})} = \underbrace{\begin{bmatrix} X_{A_{i+1}} \\ Y_{A_{i+1}} \\ 0 \end{bmatrix}}_{\mathbf{F}_{i+1}} \tag{C.10}$$

with:

$$\mathbf{U}_{i+1} = \begin{bmatrix} u_{A_{i+1}} \\ v_{A_{i+1}} \\ \theta_{i+1} \end{bmatrix} \tag{C.11}$$

Once the angle θ_{i+1} has been calculated by the 3rd equation of system C.10 using Newton Rapshon's method, its value is reinjected into the first 2 equations in order to derive the resisting forces $X_{A_{i+1}}$ and $Y_{A_{i+1}}$.

References

Acary, V., 2013. Projected event-capturing time-stepping schemes for nonsmooth mechanical systems with unilateral contact and coulomb's friction. Computer Methods in Applied Mechanics and Engineering 256, 224 – 250. URL: http://www.sciencedirect.com/science/article/pii/S0045782512003829, doi:https://doi.org/10.1016/j.cma.2012.12.012.

Avery, P., Farhat, C., 2009. The feti family of domain decomposition methods for inequality-constrained quadratic programming: Application to contact problems with conforming and nonconforming interfaces. Computer Methods in Applied Mechanics and Engineering 198, 1673 – 1683. URL: http://www.sciencedirect.com/science/article/pii/S0045782509000103, doi:https://doi.org/10.1016/j.cma.2008.12.014. advances in Simulation-Based Engineering Sciences – Honoring J. Tinsley Oden.

Belytschko, T., Mullen, R., 1978. Stability of explicit-implicit mesh partitions in time integration. International Journal for Numerical Methods in Engineering 12, 1575–1586. URL: https://onlinelibrary.wiley.com/doi/abs/10.1002/nme.1620121008, doi:10.1002/nme.1620121008, arXiv:https://onlinelibrary.wiley.com/doi/pdf/10.1002/n

Belytschko, T., Yen, H.J., Mullen, R., 1979. Mixed methods for time integration. Computer Methods in Applied Mechanics and Engineering 17-18, 259 – 275. URL: http://www.sciencedirect.com/science/article/pii/0045782579900227, doi:https://doi.org/10.1016/0045-7825(79)90022-7.

Beneš, M., Krejčí, T., Kruis, J., 2018. A feti-based mixed explicit-implicit multi-time-step method for parabolic problems. Journal of

Computational and Applied Mathematics 333, 247 – 265. URL: http://www.sciencedirect.com/science/article/pii/S0377042717305502, doi:https://doi.org/10.1016/j.cam.2017.10.041.

Beneš, M., Kruis, J., 2018. Multi-time-step domain decomposition and coupling methods for nonlinear parabolic problems. Applied Mathematics and Computation 319, 444 – 460. URL: http://www.sciencedirect.com/science/article/pii/S0096300317302783, doi:https://doi.org/10.1016/j.amc.2017.04.026. recent Advances in Computing.

Brun, M., Gravouil, A., Combescure, A., Limam, A., 2015. Two feti-based heterogeneous time step coupling methods for newmark and α-schemes derived from the energy method. Computer Methods in Applied Mechanics and Engineering 283, 130 – 176. URL: http://www.sciencedirect.com/science/article/pii/S0045782514003193, doi:https://doi.org/10.1016/j.cma.2014.09.010.

Combescure, A., Gravouil, A., 2001. A time-space multi-scale algorithm for transient structural nonlinear problems. Mécanique & Industries 2, 43 – 55. URL: http://www.sciencedirect.com/science/article/pii/S1296213900010770.

Combescure, A., Gravouil, A., 2002. A numerical scheme to couple subdomains with different time-steps for predominantly linear transient analysis. Computer Methods in Applied Mechanics and Engineering 191, 1129 –1157.

Daniel, W., 1997. Analysis and implementation of a new constant acceleration subcycling algorithm. International Journal for Numerical Methods in Engineering 40, 2841 – 2855.

Escaig, Y., Marin, P., 1999. Examples of domain decomposition methods to solve non-linear problems sequentially. Advances in Engineering Software 30, 847 – 855. URL: http://www.sciencedirect.com/science/article/pii/S0965997898001148, doi:https://doi.org/10.1016/S0965-9978(98)00114-8.

Farhat, C., Mandel, J., Roux, F.X., 1994. Optimal convergence properties of the feti domain decomposition method. Computer Methods in Applied Mechanics and Engineering 115, 365–385.

Gravouil, A., Combescure, A., 2001. A multi-time-step explicit-implicit method for non- linear structural dynamics. International Journal for Numerical Methods in Engineering 50, 199 –225.

Gravouil, A., Combescure, A., Brun, M., 2015. Heterogeneous asynchronous time integrators for computational structural dynamics. International Journal for Numerical Methods in Engineering 102, 202 –232, DOI: 10.1002/nme.4818.

Hughes, T.J., Pister, K.S., Taylor, R.L., 1979. Implicit-explicit finite elements in nonlinear transient analysis. Computer Methods in Applied Mechanics and Engineering 17-18, 159 – 182. URL: http://www.sciencedirect.com/science/article/pii/0045782579900860, doi:https://doi.org/10.1016/0045-7825(79)90086-0.

Hughes, T.J.R., Liu, W.K., 1978a. Implicit-Explicit Finite Elements in Transient Analysis: Implementation and Numerical Examples. Journal of Applied Mechanics 45, 375–378. URL: https://doi.org/10.1115/1.3424305, doi:10.1115/1.3424305, arXiv:https://asmedigitalcollection.asme.org/appliedmechanics/article-pdf/45/2/3

Hughes, T.J.R., Liu, W.K., 1978b. Implicit-Explicit Finite Elements in Transient Analysis: Stability Theory. Journal of Applied Mechanics 45, 371–374. URL: https://doi.org/10.1115/1.3424304, doi:10.1115/1.3424304, arXiv:https://asmedigitalcollection.asme.org/appliedmechanics/article-pdf/45/2/3

Klisinski, M., Moström, A., 1998. On stability of multitime step integration procedures. Journal of Engineering Mechanics 124, 783–793. URL: https://ascelibrary.org/doi/abs/10.1061/28ASCE290733-9399281998291243A72878329, doi:10.1061/(ASCE)0733-9399(1998)124:7(783), arXiv:https://ascelibrary.org/doi/pdf/10.1061/28ASCE290733-9399281998291243A7287

Liu, W., Belytschko, T., 1982. Mixed-time implicit-explicit finite elements for transient analysis. Computers & Structures 15, 445 – 450. URL: http://www.sciencedirect.com/science/article/pii/0045794982900797, doi:https://doi.org/10.1016/0045-7949(82)90079-7.

Mazars, J., Grange, S., M., B., 2018. Simplified modeling strategy for the thermomechanical analysis of massive reinforced concrete structures at an early age. Appl. Sci 8, 448.

Simo, J., Hughes, T., 1998. Computational Inelasticity. Mechanics and materials, Springer Interdisciplinary applied mathematics, vol.7.

Smolinski, P., 1992a. An explicit multi-time step integration method for second order equations. Computer Methods in Applied Mechanics and Engineering 94, 25 – 34. URL: http://www.sciencedirect.com/science/article/pii/004578259290155D, doi:https://doi.org/10.1016/0045-7825(92)90155-D.

Smolinski, P., 1992b. Stability analysis of a multi-time step explicit integration method. Computer Methods in Applied Mechanics and Engineering 95, 291 – 300. URL: http://www.sciencedirect.com/science/article/pii/004578259290188P, doi:https://doi.org/10.1016/0045-7825(92)90188-P.

Wriggers, P., 2006. Computational Contact Mechanics. Springer-Verlag Berlin Heidelberg. doi:10.1007/978-3-540-32609-0.

Wu, Y., Smolinski, P., 2000. A multi-time step integration algorithm for structural dynamics based on the modified trapezoidal rule. Computer Methods in Applied Mechanics and Engineering 187, 641 – 660. URL: http://www.sciencedirect.com/science/article/pii/S0045782599003436, doi:https://doi.org/10.1016/S0045-7825(99)00343-6.

Graphical Abstract

Implicit coupling of heterogeneous and asynchronous time-schemes using a primal approach based on velocity continuity at the sub-domain interface

Stéphane Grange, David Bertrand

Highlights

Implicit coupling of heterogeneous and asynchronous time-schemes using a primal approach based on velocity continuity at the sub-domain interface

Stéphane Grange, David Bertrand

- Research highlight 1: A primal coupling algorithm based on a velocity gluing at the interface for implicit problems is introduced.
- Research highlight 2: The tangent algorithm operator is derived even for multi-time stepping (i.e. asynchronous) and for various integration schemes using different integration parameters and order approximation (i.e. heterogeneous).